(1)

8/16/94 Final Technical (6/1/91 to 3/31/94)

Design of New Multi-Functional Electroactive Polymers With Emphasis on Optical Nonlinearity

F49620-91-C-0054
63218C
1601-06

Larry R. Dalton

University of Southern California
Department of Chemistry
Los Angeles, California 90089-1062

AFOSR-TR- 94 0549

AFOSR/NL
Building 410, Bolling Air Force Base, DC
20332-6448

Dr. Lee

Approved for Public Release: Distribution Unlimited

Synthesis and processing of organic second-order nonlinear optical materials for fabrication of electro-optic modulators are discussed. Topics dealt with in order include (1) synthesis of chromophores characterized by large hyperpolarizability and good thermal stability, (2) covalent coupling of nonlinear optical chromophores to polymer lattices, (3) lattice hardening reactions which permit locking-in of electric field poling-induced macroscopic noncentrosymmetric order, (4) fabrication of buried channel nonlinear optical waveguides by photochemical and reactive ion etching techniques, (5) coupling of nonlinear optical waveguides to fibe· optic transmission lines and drive electronics, (6) prototype device fabrication and evaluation. Various device configurations are reviewed and recent advances in applications are discussed. Comparison is made between the performance of organic and inorganic materials for electro-optic modulation applications

Electro-optic modulation, nonlinear optical polymers, polymeric waveguides, Mach-Zehnder modulators, birefringent modulators, directional couplers, DEC chromophores

57

Unclassified Unclassified Unclassified UL

GENERAL INSTRUCTIONS FOR COMPLETING SF 298

The Report Documentation Page (RDP) is used in announcing and cataloging reports. It is important that this information be consistent with the rest of the report, particularly the cover and title page. Instructions for filling in each block of the form follow. It is important to **stay within the lines to meet optical scanning requirements.**

Block 1. Agency Use Only (Leave Blank)

Block 2. Report Date. Full publication date including day, month, and year, if available (e.g. 1 Jan 88). Must cite at least the year.

Block 3. Type of Report and Dates Covered. State whether report is interim, final, etc. If applicable, enter inclusive report dates (e.g. 10 Jun 87 - 30 Jun 88).

Block 4. Title and Subtitle. A title is taken from the part of the report that provides the most meaningful and complete information. When a report is prepared in more than one volume, repeat the primary title, add volume number, and include subtitle for the specific volume. On classified documents enter the title classification in parentheses.

Block 5. Funding Numbers. To include contract and grant numbers; may include program element number(s), project number(s), task number(s), and work unit number(s). Use the following labels:

C	- Contract	**PR**	- Project
G	- Grant	**TA**	- Task
PE	- Program Element	**WU**	- Work Unit Accession No.

Block 6. Author(s). Name(s) of person(s) responsible for writing the report, performing the research, or credited with the content of the report. If editor or compiler, this should follow the name(s).

Block 7. Performing Organization Name(s) and Address(es). Self-explanatory.

Block 8. Performing Organization Report Number. Enter the unique alphanumeric report number(s) assigned by the organization performing the report.

Block 9. Sponsoring/Monitoring Agency Names(s) and Address(es). Self-explanatory.

Block 10. Sponsoring/Monitoring Agency. Report Number. (If known)

Block 11. Supplementary Notes. Enter information not included elsewhere such as: Prepared in cooperation with...; Trans. of ..., To be published in .... When a report is revised, include a statement whether the new report supersedes or supplements the older report.

Block 12a. Distribution/Availablity Statement. Denote public availability or limitation. Cite any availability to the public. Enter additional limitations or special markings in all capitals (e.g. NOFORN, REL, ITAR)

DOD	- See DoDD 5230.24, "Distribution Statements on Technical Documents."
DOE	- See authorities
NASA	- See Handbook NHB 2200.2.
NTIS	- Leave blank.

Block 12b. Distribution Code.

DOD	- DOD - Leave blank
DOE	- DOE - Enter DOE distribution categories from the Standard Distribution for Unclassified Scientific and Technical Reports
NASA	- NASA - Leave blank
NTIS	- NTIS - Leave blank.

Block 13. Abstract. Include a brief (Maximum 200 words) factual summary of the most significant information contained in the report.

Block 14. Subject Terms. Keywords or phrases identifying major subjects in the report.

Block 15. Number of Pages. Enter the total number of pages.

Block 16. Price Code. Enter appropriate price code (NTIS only).

Blocks 17. - 19. Security Classifications. Self-explanatory. Enter U.S. Security Classification in accordance with U.S. Security Regulations (i.e., UNCLASSIFIED). If form contains classified information, stamp classification on the top and bottom of the page.

Block 20. Limitation of Abstract. This block must be completed to assign a limitation to the abstract. Enter either UL (unlimited) or SAR (same as report). An entry in this block is necessary if the abstract is to be limited. If blank, the abstract is assumed to be unlimited.

COMPLETED PROJECT SUMMARY

TITLE: Design of New Multi-Functional Electroactive Polymers With Emphasis on Optical Nonlinearity

PRINCIPAL INVESTIGATOR: Professor Larry R. Dalton
Loker Hydrocarbon Research Institute
Departments of Chemistry and of Materials Science & Engineering
University of Southern California
Los Angeles, California 90089-1661

INCLUSIVE DATES: 1 June 1991 to 31 March 1994

CONTRACT NUMBER: F49620-91-C-0054

PERSONNEL: See following pages.

PUBLICATIONS: See following pages.

ABSTRACT OF OBJECTIVES AND ACCOMPLISHMENTS:

The following objectives were defined and pursued: (1) synthesis of chromophores characterized by large hyperpolarizability and good thermal stability, (2) covalent coupling of nonlinear optical chromophores to polymer matrices, (3) lattice hardening reactions which permit locking-in of electric field poling-induced macroscopic noncentrosymmetric order, (4) fabrication of buried channel nonlinear optical waveguides by photochemical and reactive ion etching techniques, (5) coupling of nonlinear optical waveguides to fiber optic transmission lines and drive electronics, (6) prototype device fabrication and evaluation. Substantial progress was made in achieve all objectives as is attested to by the 63 publications deriving from this work and by the progress report which follows setting this work in perspective with other efforts in the field of organic nonlinear optics and comparing results to those obtained with competitive materials, e.g., inorganic electro-optic modulator materials.

Publications Deriving From Contract Support

1. W. H. Steier, Y. Shi, L. P. Yu, M. Chen, and L. R. Dalton, "Nonlinear Optics and Optical Micro-patterning in Polymers with Disperse Red 19 Sidegroups," Proc. SPIE, 1775, 379-90 (1992).
2. L. R. Dalton, L. P. Yu, M. Chen, L. S. Sapochak and C. Xu, "Recent Advances in the Development and Characterization of Nonlinear Optical Materials: Second Order Materials," Synth. Met., 54, 155-60 (1992).
3. M. Chen, L. R. Dalton, L. P. Yu, Y. Q. Shi, and W. H. Steier, "Thermosetting Polyurethanes with Stable and Large Second-Order Optical Nonlinearity," Macromolecules, 25, 4032-5 (1992).
4. L. S. Sapochak, M. R. McLean, M. Chen, L. P. Yu and L. R. Dalton, "New Routes to Large Optical Nonlinearites," Proc. SPIE, 1665, 199-211 (1992).
5. L. S. Sapochak, M. R. McLean, M. Chen, and L. R. Dalton, "Multi-functional NLO Materials: New Mechanisms for NLO Effects," Proc. SPIE, 1626, 431-9 (1992).
6. Y. Shi, W. H. Steier, M. Chen, L. P. Yu and L. R. Dalton, Thermosetting Nonlinear Optical Polymer: Polyurethane with Disperse Red 19 Side Groups, Appl. Phys. Lett., 60, 2577-9 (1992).
7. C. Xu, B. Wu, L. R. Dalton, Y. Shi, P. M. Ranon, and W. H. Steier, "Novel Double-End Crosslinkable Chromophores For Second-Order Optical Nonlinearity," Macromolecules, 25, 6714-5 (1992).
8. C. Xu, B. Wu, L. R. Dalton, Y. Shi, P. M. Ranon and W. H. Steier, "New Random Main Chain, Second-Order Nonlinear Optical Polymers", Macromolecules, 25, 6716-8 (1992).
9. L. R. Dalton, "Fresh Start for Photonics," Nature, 359, 269-70 (1992)--invited article.

10. L. P. Yu, D. W. Polis, F. Xiao, L. S. Sapochak, M. R. McLean, L. R. Dalton, C. W. Spangler, T. J. Hall and K. O. Havelka, "Development of Material With Enhanced Optical Nonlinearity by Control of Ultrastructure," Polymer, 33, 3239-44 (1992).
11. C. W. Spangler, P. K. Liu, T. J. Hall, D. W. Polis, L. S. Sapochak and L. R. Dalton, " The Design of New Copolymers for $\chi^{(3)}$ Applications," Polymer, 33, 3942-50 (1992).
12. C. W. Spangler, P. Bryson, P. K. Liu, and L. R. Dalton, "Protonic Doping of Bis-Thienyl Polyenes and Oligomers of Poly[2,5-Thienylene Vinylene]: Comparison to Oxidative Doping," J. Chem. Soc. Chem. Commun., 253-4 (1992).
13. C. W. Spangler, L. Picchiotti, P. Bryson, K. O. Havelka, and L. R. Dalton, "Competition Between Polaronic and Bipolaronic Charge States in the Oxidative and Protonic Doping of Model Oligomers of Poly(dialkoxyphenylene vinylene)", J. Chem. Soc. Chem. Commun., 145-6 (1992).
14. L. R. Dalton, "Synthesis of Metallated and Metal-Free π-Electron Polymers for Nonlinear Optical Applications," Polym. Preprints, 33, 371-2 (1992).
15. S. T. Wu, J. D. Margerum, B. H. Meng, L. R. Dalton, C. S. Hsu and S. H. Lung, "Room Temperature Diphenyl-diacetylene Liquid Crystals," Appl. Phys. Lett., 61, 630-2 (1992).
16. L. S. Sapochak, F. Strohkendl, L. R. Dalton, N. Tang, J. P. Partanen, R. W. Hellwarth, T. Y. Chang, C. W. Spangler, and Q. Lin, "Excited State Dynamics Studies of Resonance Enhanced Optical Nonlinearity in Ladder Chromophores by Degenerate Four Wave Mixing," in Organic Materials for Nonlinear Optics III (OMNO III), Royal Society of Chemistry, London, 1992, pp. 283-8.
17. E.G. Nickel, C.W. Spangler, N. Tang, R.W. Hellwarth, and L.R. Dalton, "Third Order Nonlinearity in Polymer Models and Composites Containing Stabilized Bipolarons," in Organic Materials for Nonlinear Optics III, Royal Society of Chemistry, London, 1992, pp. 237-42.
18. M.L. Sachtleben, C.W. Spangler, N. Tang, R.W. Hellwarth, and L.R. Dalton, "Third Order Nonlinearity in Bis-Ferrocenyl Polyenes." in Organic Materials for Nonlinear Optics III, Royal Society of Chemistry, London, 1992, pp. 231-6.
19. C. W. Spangler, M. He, J. Laquindanum, N. Tang, R. Hellwarth, and L. R. Dalton, "Charge State Generation in Polyacetylene Model Systems: Bis-Thienyl Polyenes Incorporating Solubilizing Substituents," Polymer Preprints, 34, 384 (1993).
20. L. R. Dalton, L. S. Sapochak, and L. P. Yu, "Recent Advances in Nonlinear Spectroscopy and Nonlinear Optical Materials," J. Phys. Chem., 97, 2871-83 (1993).
21. Y. Shi, P. M. Ranon, W. H. Steier, C. Xu, B. Wu, and L. R. Dalton, "Improving the Thermal Stability by Anchoring Both Ends of Chromophores in the Side-Chain Nonlinear Optical Polymers," Appl. Phys. Lett., 63, 2168-70 (1993).
22. C. Xu, B. Wu, L. R. Dalton, P. M. Ranon, Y. Shi, and W. H. Steier, "New Cross-Linkable Polymers with Second-Order Nonlinear Optical Chromophores in the Main Chain," Proc. SPIE, 1852, 198-205 (1993).
23. C. Xu, B. Wu, M. W. Becker, L. R. Dalton, P. M. Ranon, Y. Shi, and W. H. Steier, "Main-Chain Second-Order Nonlinear Optical Polymers: Random Incorporation of Amino-Sulfone Chromophores," Chemistry of Materials, 5, 1439-44 (1993).
24. C. Xu, B. Wu, O. Todorowa, L. R. Dalton, Y. Shi, P. M. Ranon, and W. H. Steier, "Stabilization of the Dipole Alignment of Poled Nonlinear Optical Polymers by Ultrastructure Synthesis," Macromolecules, 26, 5303-9 (1993).
25. C. Xu, M. W. Becker, B. Wu, L. R. Dalton, Y. Shi, P. M. Ranon, and W. H. Steier, "Techniques for Ultrastructure Synthesis: Stabilization of Large Second-Order Optical Nonlinearities of Poled Polymers," Proc. SPIE, 2025, 20-30 (1993).
26. Y. Shi, P. M. Ranon, W. H. Steier, C. Xu, B. Wu, and L. R. Dalton, "Anchoring Both Ends of the Chromophore in the Side Chain Nonlinear Optical Polymers for Improved Thermal Stability," Proc. SPIE, 2025, 106-16(1993).
27. W. H. Steier, Y. Shi, P. M. Ranon, C. Xu, B. Wu, L. R. Dalton, W. Wang, D. Chen, and H. Fetterman, "Waveguide Photonic Devices Made From Thermally Crosslinked Second-Order Nonlinear Optical Polymers," Proc. SPIE, 2025, 535-46 (1993).
28. L. R. Dalton, L. S. Sapochak, M. Chen, and L. P. Yu "Ultrastructure Concepts of Optical Integrated Microcircuits and Polymeric Materials," in Molecular Electronics and Molecular Electronic Devices, Vol. 2, ed., K. Sienicki (CRC Press, Boca Raton, 1993) pp.125-208.
29. D. K. Dimov, L. R. Dalton, and T. E. Hogen-Esch, "Anionic Polymerization of Azo Substituted Methacrylates," Polymer Preprints, 34, 126 (1993).
30. L. R. Dalton, L. S. Sapochak, and L. P. Yu, "Recent Advances in Nonlinear Spectroscopy," J. Photochem. Photobiol. A, 71, 1-13 (1993).

31. P. M. Ranon, Y. Shi, W. H. Steier, C. Xu, B. Wu, and L. R. Dalton, "Efficient Poling and Thermal Crosslinking of Randomly Bonded Main-Chain Polymers for Stable Second-Order Nonlinearities," Appl. Phys. Lett, 62, 2605-7 (1993).
32. F. P. Strohkendl, D. J. Files, and L. R. Dalton, "Highly Stable Amplification of Femtosecond Pulses," J. Opt. Soc. Am. B, 11, 742-9 (1994).
33. L. R. Dalton, C. Xu, B. Wu, and A. W. Harper, "Techniques for Ultrastructure Synthesis: Preparation of Second Order Nonlinear Optical Materials," in Frontiers of Polymer Research, eds. P. N. Prasad and J. Nigam (Plenum, New York, 1994) pp. 175-186.
34. M. W. Becker, L. S. Sapochak, L. R. Dalton, Y. Shi, W. H. Steier, and A. K. Jen, "Large and Stable Nonlinear Optical Effects for a Polyimide Covalently Incorporating an NLO Chromophore," Chemistry of Materials, 6, 104-6 (1994).
35. B. Wu, C. Xu, L. R. Dalton, S. Kalluri, Y. Shi, and W. H. Steier, "Second-Order Nonlinear Optical Polymers With Different Chromophore Arrangements," Materials Research Society Symposium Proceedings, Vol. 328, Electrical, Optical and Magnetic Properties of Organic Solid State Materials (Materials Research Society, Pittsburgh, 1994) pp. 529-34.
36. C. Xu, B. Wu, L. R. Dalton, Y. Shi, P. M. Ranon, S. Kalluri, and W. H. Steier, "Realization of Large, Stable Second Order Optical Nonlinearities Through Double-End Crosslinkable Chromophores," Materials Research Society Symposium Proceedings, Vol. 328, Electrical, Optical and Magnetic Properties of Organic Solid State Materials (Materials Research Society, Pittsburgh, 1994) pp. 461-6.
37. J. B. Caldwell, R. W. Cruse, K. J. Drost, V. P. Rao, A. K-Y. Jen, K. Y. Wong, Y. M. Cai, R. M. Mininni, J. Kenney, E. Binkley, L. R. Dalton, Y. Shi, and W. H. Steier, "Sol-Gel-Derived Thin Films Incorporating an Organic Second-Order NLO Compound With Large bm," Materials Research Society Symposium Proceedings, Vol. 328, Electrical, Optical and Magnetic Properties of Organic Solid State Materials (Materials Research Society, Pittsburgh, 1994) pp. 535-40.
38. C. W. Spangler, M. Q. He, J. Laquindanum, L. R. Dalton, N. Tang, J. Partanen, and R. W. Hellwarth, "Bipolaron Formation and Nonlinear Optical Properties in Bis-Thienyl Polyenes," Materials Research Society Symposium Proceedings, Vol. 328, Electrical, Optical and Magnetic Properties of Organic Solid State Materials (Materials Research Society, Pittsburgh, 1994) pp. 655-60.
39. A. F. Garito, A. K-Y. Jen, C. Y-C. Lee, and L. R. Dalton, Eds, Materials Research Society Symposium Proceedings, Vol. 328, Electrical, Optical and Magnetic Properties of Organic Solid State Materials (Materials Research Society, Pittsburgh, 1994) pp. 1-817.
40. C. W. Spangler, P. K. Liu, J. Laquindanum, L. S. Sapochak, L. R. Dalton, and R. S. Kumar, "Incorporation of Ladder Polymer Subunits in Formal Copolymers for Third Order NLO Applications," in Frontiers of Polymer Research, eds. P. N. Prasad and J. Nigam (Plenum, New York, 1993).
41. C. W. Spangler, M. He, E. Nickel, J. Laquindanum, L. R. Dalton, N. Tang, and R. W. Hellwarth, "The Design of New Organic Materials with Enhanced Nonlinear Optical Properties," Mol. Cryst. Liq. Cryst., 240, 17-23 (1994).
42. B. Wu, C. Xu, Y. Ra, L. R. Dalton, S. Kalluri, Y. Shi, and W. H. Steier, "Cross-Linkable Nonlinear Optical Polymers Based on Functionalized Amino-Nitro Azobenzene," Polymer Preprints, 35, 494-5 (1994).
43. C. W. Spangler, M. He, P.-K. Liu, E. Nickel, J. Laquindanum, and L. R. Dalton, "The Design of New Organic Materials With Enhanced Nonlinear Optical Properties: Incorporation of Bipolaronic Charge Transfer," Nonlinear Optics, in press.
44. L. R. Dalton, C. Xu, B. Wu, and A. K.-Y. Jen, "Development and Application of Organic Electro-Optic Modulators," Nonlinear Optics, in press.
45. A. K.-Y. Jen, V. P. Rao, K. J. Drost, Y. M. Cai, R. M. Mininni, J. T. Kenney, E. S. Binkley, L. R. Dalton, and S. R. Marder, "Progress on Heteroaromatic Chromophores in High Temperature Polymers for Electro-optic Applictions," Proc. SPIE, 2143, 321-40(1994).
46. H. B. Meng, L. R. Dalton, and S. T. Wu, "Synthesis and Physical Properties of Asymmetric Diphenyldiacetylenic Liquid Crystals," Mol. Cryst. Liq. Cryst., in press.
47. A. K.-Y. Jen, K. J. Drost, Y. Cai, V. P. Rao, and L. R. Dalton, "Thermally Stable Nonlinear Optical Polyimides: Synthesis and Electro-Optic Properties," J. Chem. Soc., Chem. Commun., 965 (1994).
48. S. Kalluri, W. H. Steier, Z. Yang, C. Xu, B. Wu, L. R. Dalton, Y. Shi, and J. H. Bechtel, "Enhancement of Electro-Optic Properties and Temperature Stability in Sol-Gel Polymer Thin Films," Proc. SPIE, 2285 (1994).
49. S. Kalluri, W. H. Steier, C. Xu, B. Wu, M. W. Becker, Z. Yang, L. R. Dalton, Y. Shi, and J. H. Bechtel, "Improved Second Order Nonlinear Optical Polymers by Covalent Attachement-Comparison of Four Different Thermally Stable Systems," Proc. IEEE, submitted.
50. Y. Shi, J. H. Bechtel, S. Kalluri, W. H. Steier, C. Xu, B. Wu, and L. R. Dalton, "Measurement of Electro-Optic Coefficient Dispersion in Poled Nonlinear Optical Polymer Thin Films," Proc. SPIE, 2285 (1994).

51. A. K.-Y. Jen, K. Drost, V.P. Rao, Y. M. Cai, R. M. Mininni, J. Kenney, E. Binkley, L. R. Dalton, and C. Xu, "Highly Active and Thermally Stable Electro-Optic Polymers," Proc. SPIE, 2285 (1994).
52. S. Gilmour, R. A. Montgomery, S. R. Marder, L.-T. Cheng, A. K.-Y. Jen, Y. M. Cai, J. W. Perry, and L. R. Dalton, "Synthesis of Diarylthiobarbituric Acid Chromophores With Enhanced Second-Order Optical Nonlinearities and Thermal Stabilty," submitted to Chemistry of Materials.
53. L. R. Dalton, A. W. Harper, B. Wu, R. Ghosn, J. Laquindanum and J. Liang, "Polymeric Electro-Optic Modulators: From Basic Research to Commercialization," an invited article for Acta Polymerica, 1994.
54. A. Jen, K. Drost, V. Rao, Y. Cai, Y. Liu, R. Mininni, J. Kenney, E. Binkley, L. Dalton, C. Xu, and S. Marder, "The Incorporation of Highly Active and Thermally Stable Hetero-Aromatic Chromophores into High Temperature Polyimides for E-O Applications," Polymer Preprints, 35, 130-1 (1994); to be published in Nonlinear Optical Polymers: From Molecules to $\chi^{(2)}$ Applications, ACS Symposium Series (G. A. Lindsay and K. D. Singer, eds).
58. L. R. Dalton, B. Wu, A. Harper, R. Ghosn, Y. Ra, Z. Liang, R. Montgomery, S. Kalluri, Y. Shi, W. H. Steier, A. K.-Y. Jen, "Techniques of Ultrastructure and Chromophore Synthesis Relevant to the Fabrication of High Frequency Electro-Optic Modulators," Polymer Preprints, 35, 128-9 (1994); to be published in Nonlinear Optical Polymers: From Molecules to $\chi^{(2)}$ Applications, ACS Symposium Series (G. A. Lindsay and K. D. Singer, eds).
59. M. Ziari, W. H. Steier, L. R. Dalton, Y, Shi, W. Wang, D. Chen, and H. R. Fetterman, "Electrooptic Polymer Waveguide Fabrication," Polymer Preprints 35, 227-8 (1994); to be published in Nonlinear Optical Polymers: From Molecules to $\chi^{(2)}$ Applications, ACS Symposium Series (G. A. Lindsay and K. D. Singer, eds).
60. L. R. Dalton, R. Ghosn, A. W. Harper, W. H. Steier, H. Fettermanm, R. Mustacich, A. K.-Y. Jen, and K. Shea "Synthesis and Processing of Improved Second Order Nonlinear Optical Materials for Fabrication of Electro-Optic Modulaotrs," Chemistry of Materials, (1994), invited article.
61. Z. Yang, C. Xu, B. Wu, L. R. Dalton, S. Kalluri, W. H. Steier, Y. Shi, and J. H. Bechtel, "Anchoring Both Ends of Chromophores into Sol-Gel Networks for Large and Stable Second-Order Optical Nonlinearities," Chemistry of Materials, in press.
62. H. W. Oviatt, Jr., K. J. Shea, S. Kalluri, Y. Shi, W. H. Steier, and L. R. Dalton, "Applications of Organic Bridged Polysilsesquioxane Xerogels to Nonlinear Optical Materials by the Sol-Gel Method," Chemistry of Materials, submitted.
63. S. Kalluri, Y. Shi, W. H. Steier, Z. Yang, C. Xu, B. Wu, and L. R. Dalton, "Improved Poling and Thermal Stability of Sol-Gel Nonlinear Optical Polymers," Appl. Phys. Lett., sumbitted.

Personnel Associated With Project

A. Graduate Students (partial support)

1. Mark Becker
2. Paul Bryson
3. Mai Chen
4. Darin Files
5. Rima Ghosn
6. Aaron Harper
7. Joyce Laquindanum
8. Jerome Liang
9. Betty Meng
10. Robert Montgomery
11. Youngsoo Ra
12. Linda Sapochak
13. Yongqiang Shi
14. Bo Wu
15. Chengzeng Xu

B. Theses Completed (USC Degrees)

1. Mai Chen, Ph.D.(Chemistry), 1992, "New polymers exhibiting stable and large optical nonlinearities."

2. Linda Sapochak, Ph.D.(Chemistry), 1992, "Studies of well-defined conjugated pi-electron subunits: Progress in material design for nonlinear optical applications."
3. Robert Montgomery, Ph.D.(Chemistry), 1992, "Synthesis of fused ring chromophores for nonlinear optical effects."
4. Yongqiang Shi, Ph.D.(EE), 1992, "Characterization and device applications of disperse red 19 containing second-order nonlinear optical polymers."
5. Paul Bryson, Ph.D.(Chemistry), 1993, "Electron spin resonance characterization of new delocalized pi-electron oligomers in oxidative and protonic doping."
6. Chengzeng Xu, Ph.D.(Chemistry), 1993, "Design, synthesis and characterization of novel organic nonlinear optical materials."
7. Mark Becker, M.S.(Chemistry) 1993, "A novel chromophore functionalized polyimide for nonlinear optical studies."
8. Betty Meng, Ph.D.(Chemistry), 1994, "Asymmetric diphenyldiacetylenic liquid crystals."
9. Bo Wu, Ph.D.(Chemistry), 1994, "Design, synthesis and characterization of polymeric materials with second order optical nonlinearity."

C. Postdoctoral Fellows

1. Robert Montgomery
2. Frederick Strohkendl (partial support)
3. Chengzeng Xu
4. Linda Sapochak
5. Yongqiang Shi (partial support)

D. Visiting Scholars Working on Project (No Support Provided from Federal Funds)

1. Professor Olga Todorowa, Bulgarian Academy of Sciences
2. Professor C.-S. Hsu, Department of Applied Chemistry, National Chiao Tung Univeristy, Hsinchu, Taiwan

Design of New Multi-Functional Electroactive Polymers With Emphasis on Optical Nonlinearity

L. R. Dalton
Loker Hydrocarbon Research Institute
Departments of Chemistry and of Materials Science & Engineering
University of Southern California, Los Angeles, CA 90089-1661

Abstract

Our synthesis and processing of organic second-order nonlinear optical materials for fabrication of electro-optic modulators are discussed. Topics dealt with in order include (1) synthesis of chromophores characterized by large hyperpolarizability and good thermal stability, (2) covalent coupling of nonlinear optical chromophores to polymer matrices, (3) lattice hardening reactions which permit locking-in of electric field poling-induced macroscopic noncentrosymmetric order, (4) fabrication of buried channel nonlinear optical waveguides by photochemical and reactive ion etching techniques, (5) coupling of nonlinear optical waveguides to fiber optic transmission lines and drive electronics, (6) prototype device fabrication and evaluation. Various device configurations are reviewed and recent advances in applications are discussed. Comparison is made between the performance of organic and inorganic materials for electro-optic modulation applications.

1 Introduction

There is little disagreement that a revolution in communication technology is eminent. Terms such as the "information superhighway" have become common parlance. A number of advances have been the vanguard of this revolution including development of efficient fiber optic transmission lines, improvement of diode lasers, development of new and efficient optical detectors and detector arrays, continued improvement of semiconductor electronics, development of high density memories, development of flat panel displays, improvement in information processing software and advances in systems engineering concepts.

While most of the advance in information processing has involved electronic technology, we are currently reaching the theoretical limits of conventional electronic signal processing and transmission. To achieve processing rates of greater than 50 GHz and transmission distances greater than 1 meter, optical technologies are required. The issue is not whether or not new optical technologies are required but rather what materials will be used to realize the new technologies. While inorganic (semiconductor) materials have been the basis of development of electronic technologies, it is not clear at this time whether inorganic or polymeric organic materials will provide the basis of the coming revolution in optical technologies.

Three areas of research activity (development of high density rewritable optical memories, i.e., 10-20 gigabytes on a 13 cm disc; development of "100 GHz" electro-optic modulators; and development of highly efficient light-emitting diodes for flat panel displays) particularly illustrate this competition of organic and inorganic materials. In this article, we shall focus upon the development of broadband polymeric electro-optic modulators and comparison of the performance characteristics of such modulators to those developed from inorganic materials. In particular, we will focus upon (1) modulation efficiency, (2) bandwidth, and (3) auxiliary factors such as insertion loss, signal distortion, optical damage threshold, thermal stability, cost etc. In contrast to most reviews of organic optical nonlinearity, our focus will be upon the realization of practical modulators and not simply upon definition of the

structure/function relationships necessary to achieve optimum optical nonlinearity. In particular, we will focus upon materials processing relevant to system integration, e.g., integration of polymeric modulators with transmission lines and with semiconductor electronics. Because we focus upon system integration, the relevance of polymeric modulators to practical applications, such as electronic-to-optical signal transduction in the cable television industry, signal transduction in intercomputer network communication, switching in local communication networks, phased-array radar antenna feeds, analog sensor data links, rf and microwave distribution, video security systems, and photonic detection of radar and radar signal links, should be more clear.

In the following, we divide our discussion into several topics: (1) Optimizing molecular hyperpolarizability (β) by chromophore design; (2) optimizing macroscopic nonlinearity ($\chi^{(2)}$) by ultrastructure synthesis concepts; (3) optimizing other material characteristics including lattice stability, optical quality, etc. (4) processing of buried channel nonlinear optical waveguides; (5) coupling to fiber optic transmission lines and reception of through space electromagnetic radiation; (6) system integration and prototype device evaluation.

Our focus will be upon the qualitative introduction of concepts. Thus, we will routinely use the most approximate mathematical expressions (e.g., scalar variables as approximations to tensor variables) and will focus upon the simplest empirical correlations without extensive discussion of the limitations of our approach. The reader is referred to the cited literature for more detailed and precise discussion of theory and data.

However, before we turn our attention to the issue of materials, let us briefly review some device architectures. This will also permit us to introduce nomenclature that will facilitate our discussion throughout this article.

2 Device Architectures

The electro-optic effect results in a relative phase shift, $\Delta\phi$, of a optical beam passing through an E-O material when an electric field is applied.

$$\Delta\phi = \pi n^3 r_{eff} VL/\lambda h$$

where n is the index of refraction, r_{eff} is the effective electro-optic coefficient, V is the voltage of the applied modulation (electrical) signal, L is the modulation length. h is the gap distance between electrodes, and λ is the optical wavelength. The magnitude of the effective E-O coefficient depends on the device geometry, the poling direction (if electric field poling is used to establish noncentrosymmetric order), the optical wave polarization, and the modulation scheme employed. The half-wave voltage-modulation length product is defined as

$$V_\pi L = \lambda h/n^3 r_{eff}$$

The $V_\pi L$ product is a measure of the modulation efficiency of the device. The lower the product, the higher the modulation efficiency.

A modulation of the intensity of the optical beam can be obtained either from interferometric effects or modal coupling changes due to phase modulation. Among various device architectures, integrated Mach-Zehnder interferometers, waveguide birefringent modulators and directional couplers are the most popular for high speed, broad bandwidth applications. As briefly analyzed in the following section, the modulation efficiency and the harmonic distortion are different from one to another.

2.1 Integrated Mach-Zehnder interferometer

An integrated Mach-Zehnder interferometer (see Fig. 1a) consists of two straight arms as modulation areas and two Y-branches (one splits the optical beam into two and the other combines the modulated beams together). The modulation electric field is applied to one arm or both arms to modulate the index of the waveguide and thus modulate the phase of the optical beam or beams. When the two beams combine coherently at the output (second Y branch), the interference of the two beams modulates the output intensity as (assuming no loss)

$$I_o = I_i \sin^2[(\phi_{ba} + \Delta\phi)/2]$$

where I_i and I_o are the input and output intensities, ϕ_{ba} is the phase difference between the two arms, and $\Delta\phi$ is the phase modulation produced by the E-O effect. $\Delta\phi$ is zero when the modulation (electric) field is not applied. The required phase change for 100% modulation (to switch light "on" and "off") is a modulation field that produces $\Delta\phi = \pi$, which results in

$$(V_\pi L)_{MZ} = \lambda h/n^3 r_{33}$$

In analog signal applications, a DC bias voltage is applied to one arm to adjust ϕ_{ba}, and the modulation voltage is applied to the other arm. At proper DC bias voltage with $\phi_{ba} = \pi/2$ (the quadrature point) and when the modulation signal is small (not exceeding V_π), the output optical signal is linearly proportional to the input electric signal with small third-order and higher odd-order harmonic distortion terms.

$$I_o = I_i [1 - \Delta\phi + (\Delta\phi)^3/6 - (\Delta\phi)^5/120 + ...]$$

A linearization scheme is required which is essentially the correction of the third order term. From the above equation, we need either subtract a third order term from the output intensity or add a similar term in the modulation electric signals to cancel this distortion.

2.2 Integrated birefringent E-O modulator

The integrated birefringent E-O modulator is an extension of the longitudinal bulk E-O modulator to guided optical beams. The modulator (see Fig. 1b) consists of a single mode nonlinear optical (NLO) polymer waveguide and an analyzer. When the modulation field is applied to the waveguide in the poling direction, the refractive index of the waveguide will experience different changes along different directions and therefore the birefringence of the waveguide is modulated by the electric field.

$$\Delta n(TE) = n^3 r_{13} V/2 \qquad \Delta n(TM) = n^3 r_{33} V/2$$

$$\Delta\phi(TE/TM)_{sp} = \pi\Delta nL = \pi VLh(n^3 r_{13} - n^3 r_{33})/\lambda$$

In order to obtain intensity modulation, the input beam is 45 degree polarized to excite both TE and TM modes. An analyzer converts the polarization modulation into an intensity modulation signal. The output intensity of a lossless birefringent E-O modulator is given by

$$I_o = I_i \sin^2[(\phi_{sp} + \Delta\phi_{sp})/2]$$

where ϕ_{sp} is the built-in phase delay between TE and TM modes, and $\Delta\phi_{sp}$ is the modulated phase delay. The $V_\pi L$ product is (recall that for a dipolar chromophore, $r_{33} = 3\ r_{13}$ by symmetry)

$$(V_\pi L)_{BR} = 1.5\lambda h/n^3 r_{33} = 1.5(V_\pi L)_{MZ}$$

Compared with the Mach-Zehnder modulator, the modulation efficiency of the birefringent modulator is lower since $V_\pi L$ is 1.5 times higher in the BR modulator. A birefringent modulator can be biased at its quadrature point by an external compensator. At this point and when the modulation signal is small, the harmonic distortion is the same as for a Mach-Zehnder device.

2.3 E-O directional couplers

Directional couplers (see Fig. 1c) consist of two side-by-side waveguides separated by only a few microns. The overlap of the guided waves in the two waveguides couples energy back and forth between the waveguides. When the RF (electrical) voltage is applied, the modulation is obtained by modulating either the phase difference or the coupling coefficient. A directional coupler is a four-terminal device which allows two inputs and two outputs. The information of the optical beams can be exchanged between the two waveguides. When only one input terminal is used, the output intensities of the waveguides are

$$I_1(L) = I_o \{\kappa^2/[\kappa^2 + (\Delta\beta/2)^2]\} \sin^2\{L\sqrt{[\kappa^2 + (\Delta\beta/2)^2]}\}$$

$$I_2(L) = I_o \{1 - \kappa^2/[\kappa^2 + (\Delta\beta/2)^2]\} \sin^2\{L\sqrt{[\kappa^2 + (\Delta\beta/2)^2]}$$

where κ is the coupling coefficient, $\Delta\beta$ is the phase mismatch between the two waveguides, and L is the coupling length. From the above equation, the complete power crossover occurs when $\Delta\beta = 0$ and $\kappa = (\pi/2) + m\pi$, where m = 0, 1, 2, ... To turn the coupling "off" by the applied electrical field, one requires

$$\Delta\beta L = (4m + 3)^{1/2}\pi$$

or

$$V_\pi L_c = (4m + 3)^{1/2}\lambda h/n^3 r_{33}$$

The smallest voltage required for switching occurs when m = 0, which is 1.7 times larger than that of a Mach-Zehnder device. Obviously, the response of a directional coupler has all orders of harmonic distortion terms. Linearization schemes must correct both second and third order harmonic terms.

In Table 1, we summarize the features of different electro-optic modulators.

2.4 Comparison of the performance characteristics of organic and inorganic E-O modulator materials

E-O modulators made of single crystal $LiNbO_3$ are currently the focus of designers attempting to exploit modulator technology; however, lithium niobate's performance is limited by several intrinsic materials properties. First, the E-O coefficient is limited to approximately 30 pm/V for Ti in-diffusion or 23 pm/V for annealed proton exchange. One cannot expect to increase the E-O coefficient for better performance. Second, the high dielectric constant of lithium niobate crystals results in an intrinsic bandwidth-length product of approximately 6 GHz-cm. Thus, special electrode designs must be used at high frequencies to match the velocity of the optical beam and the microwave (millimeter) drive frequency. The velocity matching in $LiNbO_3$ modulators results in a major electric field reduction inside the crystal and the half-wave voltage-modulation length product (a figure of merit) increases significantly as the device bandwidth increases as shown in Fig. 2. In a lumped circuit case, the large dielectric constant also requires high rf power to drive the electrodes, since the driving power is proportional to the dielectric constant. The link gain will be increased by a factor of eight if the lithium niobate modulator is replaced by a lumped circuit polymer modulator of the same V_π.

In Table 2, we summarize crucial performance parameters of modulators and give representative values for competitive inorganic materials. The dramatic increase in bandwidth of modulators fabricated from organic materials (> 130 GHz-cm) reflects the lower dielectric constants of these materials. Note that for organic materials, $\varepsilon \approx n^2$.

In addition to a large nonlinearity of the material, a smaller distance between modulation electrodes may improve the modulation efficiency since the field strength increases as the gap decreases with a constant applied voltage. However, for a wide bandwidth E-O modulator, the electrical gap size is determined by the waveguide dimensions and impedance matching geometry. Fiber-waveguide coupling considerations impose limitations on the waveguide dimensions. Commercial single mode 1.3 μm wavelength optical fibers have core diameters of 8-9 μm and cladding diameters on the order of 125 μm. From mode coupling theory, efficient coupling occurs when the overlap integral of the fiber mode and the waveguide mode is maximized, i.e., when the field distributions of the fiber mode and the waveguide mode are the same or very close. Thus, waveguide design must optimize the mode shape in order to reduce the insertion loss; however, when the mode pattern is too large, the gap between the modulating electrodes gets large and V_π, as well as the modulation power, increases accordingly. One needs to balance the mode matching as well as the modulation efficiency.

Of course, materials must meet the thermal requirements of device fabrication and long term operation. We summarize thermal requirements in Table 3.

Since $LiNbO_3$ is single crystalline, it cannot be readily grown on other substrates (although there have been recent attempts at growth on semidconductor substrates). Consequently, the modulator is flip-chip bonded to a subtrate or alternately the electronics, fibers, and modulators are interconnected via cables and fibers. We shall see that organic polymeric modulators have the potential for efficient and cost effective integration with semiconductors.

3 Additional Potential Applications

In this section, we mention two additional applications which currently have low probability of commercial implementation but which illustrate interesting scientific concepts and different processing considerations than the device applications discussed in the preceding section. These applications include photonic detection of electromagnetic radiation and generation of photorefractive solitons. In the latter application, the E-O chromophore is only a part of the system required for a photorefractive effect; however, many of the processing considerations developed for E-O modulator applications are relevant to this application.

3.1 Photonic detection of electromagnetic radiation

A primary reason for employing photonics with low dielectric materials, in place of metallic components of conventional sensing systems, is to reduce field perturbations. Although an ideal photonic sensor would be comprised completely of low dielectric components, metallic antennas are traditionally attached to the electro-optic modulator of a photonic system to enhance field gain. Hilliard and coworkers [1] have proposed employing a low dielectric (polystyrene polymer) Luneburg lens to achieve the necessary gain; thus, they propose a completely low-dielectric electromagnetic field sensor.

Photonic electromagnetic field sensors consist of a laser source providing an optical signal which is sent through an electro-optic modulator and then to a photodetector/amplifier via optical fiber transmission lines. As already discussed, the information content (frequency, amplitude, phase) of the radiofrequency field passing through an E-O modulator can be transferred by the Pockel effect to light passing through the modulator. The modulated optical signal is converted to an electrical signal by the photodetector and is amplified to produce an RF output directly proportional to the measured field. Usually some form of amplification is required to increase the rf field strength to a sufficient level to permit reasonable modulation efficiency; here we will focus upon amplification employing a low dielectric Luneburg lens. A Luneburg lens is a spherically-shaped, broadband dielectric device that focuses an incident planar electromagnetic wave entering one side of the lens onto a spot on the opposite side of the lens. The dielectric constant of the Luneburg lens varies quadratically with the radius from a maximum value of 2 at the center of the lens to a minimum value of 1 at the lens surface, according to $\varepsilon_r = 2 - (r/a)^2$ where ε_r is the relative dielectric constant of the lens, r is the radial location within the lens, and a is the radius of the lens. In practice, the Luneburg lens is often implemented in concentric shells of polystyrene, each shell comprising a continuous dielectric constant.

Electro-optic modulator sensors can be placed on the surface of a Luneburg lens either as single elements or as units consisting of two mutually orthogonal modulators (for detecting polarization of the electromagnetic wave front). The angle-of-arrival of the electromagnetic wave fronts is determined by noting which sensors are most strongly modulated. E-O modulators can be placed over the entire surface of the lens to provide 4π steradian angle-of-arrival coverage or placed over a subsection of the lens surface to provide a narrower field-of-view. In the case of 4π steradian coverage, aperture blockage, which would occur with metal antennas, is reduced because the modulators covering the lens surface on the side of field incidence are effectively transparent to the fields. This allows fields to penetrate into the lens and be focused onto the modulators on the opposite side.

Maximum energy coupling into the E-O modulator can be achieved by minimizing the reflection of fields at the surface of the modulator. The amount of field energy passing from

the Luneburg lens to the modulator can be quantified by the reflection coefficient of the materials comprising the lens and modulator. The reflection coefficient for fields in dielectric media passing from medium 1 into medium 2 (at a planar interface, each with a relative dielectric constant of ε_{r1} and ε_{r2}) is

$$\rho = [(\varepsilon_{r1})^{1/2} - (\varepsilon_{r2})^{1/2}]/[(\varepsilon_{r1})^{1/2} + (\varepsilon_{r2})^{1/2}]$$

Although the lens/modulator interface is not a planar surface, the above equation is a good approximation at microwave and millimeter wave frequencies. The relative dielectric constant of a common inorganic E-O modulator material, e.g., $LiNbO_3$, ranges from 28 to 80. Assuming a value of 30, the reflection coefficient for fields passing from the lens surface to the modulator is 0.7. The percentage of incident energy density reflected to the source, $|\rho|^2$, is about 50%. Organic polymers have the lowest dielectric constant (approximately 3 to 3.5) of all known E-O materials resulting in about 7% reflected energy density. Moreover, organic polymers are manufacturable as thin films which make them capable of being conformably interfaced to the spherical surface of the Luneburg lens.

3.2 E-O polymers and photorefractive solitons

Solitons are solitary waves that propagate with unchanging spatial profiles. In the case of optical solitons, diffraction effects (which are the main source of distortions for normal optical waves) are canceled by nonlinear optical effects. Thus, solitons permit data to be sent over long distances without introduction of distortions or errors.

Recently, Yariv and coworkers [2] have demonstrated a new type of soliton, which uses self-trapping caused by photorefractive processes to confine light spatially. Since the magnitude of the photorefractive response is independent of the input light intensity, photorefractive solitons can be generated at relatively low light intensities, e.g., $1W/cm^2$. Photorefractive solitons will be unaffected by absorption or gain.

Creation of photorefractive solitons is a four part process. Initially, pairs of spatial frequency modes of a single input beam interfere within the photorefractive material to produce a periodic intensity distribution. The input light causes impurities (inorganics) or electron donor/acceptors (organics) to release charges (electrons or holes) which migrate toward the dark regions of the materials and become trapped. This results in a periodic charge distribution in the material which, in turn, yields a periodic electrical field which is phase shifted by $\pi/2$ from the original light interference pattern if no external electric field is present. Finally, the induced space-charge field alters the refractive index periodically through the linear E-O effect. The index of refraction grating created in this manner couples the intensities of the spatial frequency modes and introduces a nonlinear phase for each mode. The strength of the coupling and magnitude of the nonlinear phase are dependent on the properties of the photorefractive material and the electric field present within the material. The nonlinear phase change of each spatial frequency mode is responsible for confinement of the input laser beam.

Of course, a variety of conditions must be satisfied for the generation of photorefractive solitons. First, energy exchange between the interfering spatial modes must be minimized. The transverse profile of a photorefractive soliton is unchanged in the presence of absorption or gain only if all spatial frequency components are effected equally. The coupling between the intensities of the spatial modes is minimized when the induced index grating is in-phase with the light interference pattern. The phase of the refractive index

grating can be controlled by applying an external DC electric field. Since the period of the light interference pattern is large, the intensity coupling remains small for a range of magnitudes of the external field. Second, the magnitude of the photorefractive focusing must exactly match the strength of the diffraction effects. This can be accomplished by varying the strength of the external electric field, which varies the magnitude of the electro-optic effect within the material. Finally, the input light must have a spatial frequency mode distribution which allows soliton formation.

Observation of photorefractive solitons by Yariv and coworkers [2] was made employing inorganic crystals. A similar photorefractive phenomena should be observable in E-O photorefractive polymers existing either as composites [3] or as homopolymers [4].

4 Synthesis and processing of materials for electro-optic modulator applications

From the discussion presented in the two preceding sections, it should be clear that somewhat different processing is required for different applications; in particular, photonic detection of electromagnetic radiation requires significantly less complicated processing and has less demanding materials requirements than signal transduction for cable television applications. In the following discussion, we focus upon representative synthesis and processing conditions which will likely be required for significant commercialization of electro-optic modulators.

We restrict our consideration to polymeric materials although single crystal organic materials could, at least in principle, be used in the fabrication of electro-optic modulators analogous to the use of single crystal inorganic materials such as lithium niobate. In can be noted that the highest reported optical nonlinearities for second-order organic materials have been for crystals (e.g., r_{11} = 400 pm/V for 4'-dimethylamino-N-methyl-4-stilbazolium tosylate [5]). However, currently known organic crystals are unsuitable for commercial applications and it is not clear that crystal growing methodologies and circuit integration technologies can be developed to permit the incorporation of such materials into devices in the near future. At this point in time, polymeric organic NLO materials are clearly the organic materials of choice for the fabrication of E-O devices and thus will be our focus.

4.1. Optimization of molecular optical nonlinearity

When we speak of optical nonlinearity to be exploited for electro-optic modulation applications, we are, at least ideally, speaking of purely non-resonant optical nonlinearity. Only virtual excitations contribute to such nonlinearity and the response time should be the phase relaxation time rather than a state lifetime. In reality the best we can do is to approximate this situation by employing carrier electromagnetic radiation (light) and modulation radiation far removed from material optical resonant frequencies. Our discussion of the theory of hyperpolarizability will focus upon nonresonant optical nonlinearity.

As an aside, we note that Garito [6] has demonstrated an interesting enhancement of optical nonlinearity based upon exploiting the hyperpolarizabilities associated with populated excited states. Because of the potential problems associated with heating, optical loss, response time (associated with the excited state lifetime) and the requirement of a control beam, we do not pursue the discussion of the exploitation of such optical nonlinearities for device applications.

With the exception of octupolar [7] chromophores, organic second-order nonlinear optical materials have been prepared from dipolar chromophores of the following general form:

(electron donor)-(π electron connective segment)-(electron acceptor)

It would seem that the logical way to define structure/function relationships required for the optimization of optical nonlinearity would be to carry out appropriate quantum mechanical calculations and indeed considerable research effort has been expended on such activities [8]. However, since optical nonlinearity (electronic hyperpolarizability) depends upon electron coulomb correlations and electronic excited states, it is not surprising that the quantitative reliability of such calculations is not as good as for the calculation of molecular geometry or ground state energy. Calculations have been of substantial utility in predicting trends and for gaining physical insight. Marder and Perry [9] have been particularly successful in using simple (two level) calculations to guide synthetic efforts aimed at optimizing molecular hyperpolarizabilities.

Stated simply, Marder and Perry emphasize that optical nonlinearity can be enhanced by (1) maintaining good electron correlation in the connective (bridge) segment and by (2) avoiding loss of electron correlation in both the ground (e.g., neutral form) and excited (e.g., charge separated) state (of the simple two state model of nonlinearity). Maintaining good electron correlation in the connective segment can, for example, be accomplished by minimizing bond length alternation in polyene connective segments. This is an observation that was also realized in the study of electrically conducting π-electron polymers. Optimizing electron correlation in the connective segments may, however, not be appropriate for other reasons. First of all, optical gap and bond length alternation are correlated with the result that optical gap is in turn correlated to molecular hyperpolarizability or optical nonlinearity (see Fig. 28 of ref. [10]). In our attempt to improve optical nonlinearity, we must be careful not to push the optical bandedge too near the operating wavelength. In this communication, we focus upon an optical operating wavelength of 1.3 microns so optical band edges of our E-O chromophore must be kept significantly below 1 micron. A second problem encountered with optimizing electron correlation in the connective segment is that of introducing chemical reactivity so that the chromophore becomes unusable because of reactivity. Attempts to maintain good electron correlation in both the ground and excited states has motivated focus upon design of electron acceptor segments which assure the retention of good electron correlation in the excited state while preserving a large difference in the dipole moments of the ground and excited states. Recall that in the two state model, hyperpolarizability depends upon the transition dipole (μ_{ge}), the difference between the dipole moments of the ground and excited state ($\mu_{ee} - \mu_{gg}$), and the optical gap (E_{ge}).

$$\beta \propto (\mu_{ee} - \mu_{gg})(\mu_{ge}^2)/E_{ge}^2$$

It is interesting to consider the development of high β chromophores from a historical perspective as done by Marder and Perry in a recent review [9a]. Throughout the 1980s, state-of-the-art organic second order chromophores largely consisted of stilbene or azobenzene moieties end-capped with electron-donating groups (such as N,N-dimethylamino) and electron-withdrawing groups (such as the nitro group). 4-N,N-dimethylamino-4'-nitrostilbene (DANS), for which $\mu\beta = 35 \times 10^{-46}$ esu, continues to be a useful reference for assessing optical nonlinearity. During this period of time, efforts to increase hyperpolarizability focused upon finding stronger donor and acceptor groups and increasing the length of the π-electron connective segment, e.g., increasing the number of

double bonds. In 1991, Marder and coworkers [8b] showed that there is an optimal combination of donor and acceptor strengths required to maximize $\mu\beta$ for a given connective segment and beyond that point, increased donor-acceptor strength leads to a diminution of hyperpolarizability. In 1993, Gorman and Marder [9c] demonstrated that hyperpolarizability could be correlated with bond length alternation. For donor-acceptor-substituted polyenes, bond length alternation is related to the relative contributions of neutral and charge separated resonance structures which is, in turn, dependent upon donor-acceptor strength. Molecules with aromatic ground states tend to be more bond length alternated than a simple polyene of comparable length--a phenomena which can be attributed to the high price in energy which must be paid upon loss of aromaticity upon polarization. Marder and coworkers enunciated two key design factors in optimizing hyperpolarizability. (1) For a chromophore which has a connective segment (bridge) that losses aromaticity upon polarization but also has an acceptor that gains aromaticity upon polarization, the bond length alternation of the bridge is reduced and a large enhancement (e.g., a factor of 40 relative to DANS) in $\mu\beta$ results [9]. Such acceptors include 3-phenyl-5-isoxazolone and thiobarbituric acid derivatives. (2) Optical nonlinearity can be enhanced by replacing benzene rings with heterocyclic rings such as thiazole or thiophene. Such structures have less aromatic stabilization energy and their use has resulted in $\mu\beta$ values 10 times DANS

A great deal of attention has also been focused upon designing chromophores with improved thermal and chemical stabilities [11]. Some synthetic modifications to improve stability are obvious, e.g., replacing polyene structures with heteroaromatic [12] and ladder type [13] structures. Tools routinely used for assessing success include thermogravimetric analysis (TGA) and differential scanning calorimetry (DSC). Twieg and coworkers [11b,c] have also employed cyclic voltammetry (CV) to gain insight into the mechanism of decomposition of chromophores. In particular, in studies of lophine and azobenzene chromophores [11b,c], they find that thermal stability correlates reasonably well with oxidation potential. Among significant observations of Twieg and coworkers [11b,c] is that the thermal stability of amine donor groups can be improved by switching from alkyl amines to aryl amines. (It is interesting to note that the decomposition temperature of azobenzene chromophores with alkyl amine donor groups is determined by decomposition of the alkyl segment and not the azo moiety as widely assumed.)

Of course, depending upon mechanism, decomposition temperature for a chromophore may vary with lattice. For example, if decomposition is by a bimolecular mechanism involving the chromophore and oxygen, then the decomposition kinetics may depend upon diffusion of oxygen in the final polymer lattice.

In Fig. 3, we list representative chromophores which have been synthesized in the search for chromophores with improved hyperpolarizability and thermal stability. In this figure, we represent hyperpolarizability relative to DANS and thermal decomposition temperature (where available).

Of course, even if a chromophore is found with large hyperpolarizability and good thermal stability, success is not assured. One must succeed in incorporating this chromophore in high concentration into an appropriate polymer lattice, must realize a high degree on noncentrosymmetric order, and must process the resulting poled polymer into a buried channel waveguide structure. All of these requirements demand a certain degree of trial and error so that a large number of chromophores must be synthesized to appropriately define all relevant structure/function relationships.

4.2 Preparation of stabilized noncentrosymmetric lattices incorporating high β chromophores

Fabrication of electro-optic devices relies upon the macroscopic second order susceptibility, $\chi^{(2)}$ which in term is related to molecular hyperpolarizability, β, by the approximate relationship

$$\chi^{(2)} = NF\beta\langle\cos^3\theta\rangle$$

The requirement of noncentrosymmetric macroscopic symmetry appears in the polar order parameter $\langle\cos^3\theta\rangle$. F contains all local field effects. As it turns out, optimization of chromophore loading (number density N) and chromophore order is not easily accomplished for high $\mu\beta$ materials. If chromophore loading could be easily optimized to point of approaching a pure chromophore lattice and if ordering efficiencies approaching perfect chromophore ordering could be achieved, it is quite clear that electro-optic coefficients in the range of hundreds of picometers per volt could be achieved with existing chromophores. For such values, the performance of second order materials begins to approach to within an order of magnitude the efficiency of liquid crystal materials in effecting modulation although the switching speed of second order materials is more than a million times faster than the switching speed of liquid crystal materials. If an electro-optic coefficient on the order of a thousand picometers per volt could be obtained, it is clear that major technological applications of second order nonlinear optical materials could be realized. For example, beam steering (spatial light modulation) applications as well as electro-optic modulation applications could be accomplished.

Unfortunately, the electrostatic repulsion between high $\mu\beta$ chromophores opposes optimization of both of these parameters. Since $\langle\cos^3\theta\rangle$ is defined by the competition between poling field-molecular dipole interactions and dipole-dipole repulsive interactions, it is not a simple matter to estimate molecular order for a given poling field unless chromophore concentrations are sufficiently low that dipole-dipole interactions are unimportant. The preceding statement can be expressed approximately in a mathematical form as

$$\langle\cos^3\theta\rangle = (\mu E_p F/5kT)(1 - L^2(W/kT))$$

where E_p is the electric poling field and L is the Langevin function. The intermolecular potential associated with chromophore-chromophore interactions can be expressed as $W\cos\phi$ where ϕ is the angle between the chromophore dipole, μ, axis and the directional field from surrounding molecules (chromophores). London [14] has shown that interaction energy between two polarizable dipoles arises from three forces; namely, the van der Waals force, the orientational force. and the induction force. The statistically averaged potential energy can be represented as [14]

$$W = 2\mu^4/(3r^6kT) + 2\mu^2\alpha/r^6 + 3I\alpha^2/4r^6$$

where r is the average distance between chromophore dipoles and I is the ionization potential. Accurate calculations using the above theory are not trivial to carry out when corona poling is employed and accurate calculations require some modeling of polymer dynamics to assess the closest approach distance. However, if representative poling fields are estimated, the approximate observation can be made that reduction of $\langle\cos^3\theta\rangle$ can be

significant for chromophore-chromophore separations of 1 nm or less. Such small separations appear not to have been achieved in composite systems due to poor solubility of the chromophore in the host polymer but can quite readily be realized for covalent incorporation of chromophores.

We have found qualitatively that dipolar repulsive interactions begin to dominate for chromophore concentrations between 40 and 75 weight percent. This statement is based upon observations of a maximum in graphs of $\chi^{(2)}$ versus chromophore concentration for covalently incorporated chromophores (where we can assume that chromophore aggregation has been avoided).

Twieg and coworkers [11b] have made the important observation that long term thermal stability correlates well with the difference between the glass transition of the final polymer matrix and the temperature at which that matrix is used. For processing temperatures on the order of 250°C and use temperatures on the order of 100°C, their data suggest that the hardened (final) polymer lattice must have a glass transition temperature greater than 300°C.

Let us review the various scenarios for achieving stabilized (high T_g) noncentrosymmetric lattices reflecting adequate values of N and $\langle\cos^3\theta\rangle$. Three general approaches have been used to achieve noncentrosymmetric second order lattices; namely, (1) exploitation of molecular self-assembly--most notably, crystal growth, incorporation into inclusion compounds, or formation of liquid crystalline (ordered) domains in the bulk material; (2) sequential synthesis exploiting Van der Waals, ionic, or covalent interactions, and (3) utilization of external force, e.g., induction of molecular order by electric field poling. We note that the preceding classification scheme is somewhat arbitrary as sequential synthesis methods obviously involve the concept of molecular self-assembly.

Molecular self-assembly [10,15] is, of course, chromophore specific and natural formation of noncentrosymmetric lattices is quite rare due to dipolar repulsion between chromophores. Moreover, coupling of organic crystals to fiber optic transmission lines and interface of organic crystals to drive electrodes in electro-optic modulators poses difficulties. Although this comment also applies to inorganic crystals such as lithium niobate, specialized techniques have been developed for lithium niobate crystals which (although costly and complicated) do permit system integration of such crystal modulators; it is not clear that these are easily adapted to organic crystals. It is also not a trivial matter to design chemical reactivities into crystalline materials which can be used to harden crystals by solid state reactions. While crystal growth continues to hold promise for some applications such as frequency doubling, this approach currently is not the method of choice for preparation of materials for electro-optic modulation applications. However, considering that electro-optic coefficients on the order of 400 pm/V at 820 nm have been measured for single crystals of the organic salt 4'-dimethylamino-N-methyl-4-stilbazolium tosylate (DAST) [5], it should be realized that a breakthrough in crystal fabrication could dramatically change the picture of application of organic nonlinear optical materials.

With ordered phases, such as liquid crystalline materials, the problem of stabilizing the phase to withstand processing into integrated devices must be overcome. Lattice hardening techniques, such as those to be shortly discussed in the consideration of poled polymers, are required.

A variety of sequential synthesis methods have been adapted to the preparation of noncentrosymmetric lattices. These include Langmuir-Blodgett methods [10,16], Merrifield-type stepwise covalent coupling reactions [10,17], stepwise ionic coupling reactions [10,18], and modified molecular beam epitaxy methods [10,19]. Sequential synthesis methods afford the advantage of permitting the preparation of thin films of precisely controlled dimensions

which can be quite useful in phase-matched second harmonic generation. However, fabrication of highly ordered films of thicknesses on the order of 1 micron becomes quite labor intensive. Thus, while sequential methods afford the possibility of very high order and the preparation of intricate and highly defined structures [10,16-19], such methods cannot currently be viewed as the method of choice for fabricating prototype electro-optic modulators. The current method of choice for the fabrication of noncentrosymmetric lattices used in electro-optic modulators appears to be electric-field poling. As with crystal growth mentioned above, a breakthrough in sequential synthesis methodology could dramatically alter the current view of preferred fabrication methods.

Electric-field poling can be applied quite generally to dipolar chromophores existing as components of polymer composites, as pendants covalently coupled to polymer backbones, or as covalently-incorporated components of polymer backbones [10,20]. Utilization of composites has the advantage of convenience as commercially available chromophores and host polymers can frequently be employed without chemical modification. Indeed, historically this was the first approach explored but it was soon realized this approach resulted in insufficient chromphore orientational stability when conventional elastomeric polymers (e.g., polymethylmethacrylate, PMMA) were employed as host lattices. More recently, composite fabrication has been revitalized by the use of high thermal stability polymer lattices such as polyimides [10,21,22].

Disadvantages of composite materials, in addition to poor coupling of the chromophore dynamics to that of the host polymer leading to relaxation of poling-induced order, include finite solubility of the nonlinear optical chromophore in the host polymer, phase separation and aggregation, sublimation of chromophores at high processing temperatures, dissolution of chromophores with application of cladding layers, and a plasticizing effect on the host lattice.

Attachment of chromophores as pendants to flexible chain polymer backbones or incorporation of chromophores as components of the polymer backbone leads to improvement in the stability of poling-induced order relative to composite materials; however, realization of stability at temperatures above ambient requires further lattice hardening reactions. Work on lattice hardening dates from the pioneering efforts of Marks and coworkers [23] and of Eich and coworkers [23] on thermosetting epoxy polymers.

In the following, we discuss three general schemes for achieving lattice hardening (T_g elevation) subsequent to effecting noncentrosymmetric order by electric field poling. These include (1) use of end-functionalized chromophores to carry out a two-step synthesis of a hardened, noncentrosymmetric lattice [24]. In the first step (polymerization reaction), a processible precursor polymer is synthesized, spin cast into an optical quality film, heated and poled. The second step consists of an addition or condensation reaction to produce a heavily-crosslinked (hardened) matrix. (2) The second approach exploits the well-known imidization reaction to achieve lattice hardening [10,20-22,24c,24e,25]. (3) The third procedure uses multi-functional chromophores to achieve a tightly coupled three-dimensional lattice. This approach can be viewed as analogous to sol-gel processing of glasses [10,20,26] or as a modification of the first procedure where steps one and two are not clearly separated.

A schematic representation of the first procedure is shown in Fig. 4. The left hand side of Fig. 4 (denoted I) shows production of a hardened lattice by exploiting asymmetric reactivities. For example, the end of the chromophore denoted "B" typically contains an electron withdrawing substituent such as a nitro or sulfonyl group and a reactive functional group such as an acrylate group. The end denoted "A" typically contains and electron donating group such as an amine group and a reactive functionality such as an amine or

hydroxyl group. Representative fabrication of a hardened lattice would involve (1) forming a processible prepolymer by addition polymerization involving the methacylate functionality; processing this prepolymer into a thin film by spin casing; and poling the film near the glass transition temperature of the prepolymer. (2) A hardened lattice is produced by a subsequent condensation (crosslinking) reaction involving the hydroxyl functionality. In part II of this figure, the chromophore is terminated at both ends by the same functionality so that a main chain prepolymer is obtained. Lattice hardening is effected by the crosslinking functionality (denoted XL) which is incorporated into the main chain of the prepolymer. This functionality may exploit either addition or condensation reactivity. It is clear that highly crosslinked matrices can be obtained by both of these approaches; a somewhat higher crosslink density may be possible with the latter approach. The effect of the final crosslinking step upon improving the stability of optical nonlinearity is shown in Fig. 5; the data shown in this figure was obtained for a polymer prepared according to the scheme shown on the left hand side of Fig. 4 [24a]. We have also found it useful to employ a dynamic assay of the thermostability of nonlinear optical activity. In Fig. 6, we show a schematic representation of the experimental arrangement used to effect such measurements; and in Fig. 7, we show representative data. In the dynamical analysis, second harmonic generation efficiency is constantly monitored as a function of increasing the sample temperature at a constant rate (typically 10°C per minute). The data shown in Fig. 7 was obtained for the same material as the data shown in Fig. 5 [24a]. Comparison of data such as shown in Fig. 7 with thermal gravimetric analysis data is useful in understanding the roles of both lattice (polymer) dynamics and lattice decomposition in loss of optical nonlinearity at elevated temperatures. Detailed analysis of dynamic NLO data such as shown in Fig. 7 is also useful in accessing the effectiveness of lattice hardening reactions. A step trace, which reflects incomplete loss of NLO activity (such as shown in Fig. 8), can be indicative of incomplete lattice crosslinking. The step nature of the curve reflects the existence of regions of the lattice with different crosslinking densities. The progress of lattice hardening can be investigated by repeating dynamic measurements on samples exposed to different reaction conditions. Such studies, together with pressure-dependence studies to assess the dependence of free volume upon crosslinking, should prove useful in both optimizing lattice hardening protocols and in assessing the limits of this approach for enhancing thermal stability of NLO lattices. As might be expected, an empirical relationship can be established between dynamic and static assays of thermal stability; long term stability is routinely observed for temperatures 30°C or more below the temperature at which loss of NLO activity is first observed in the dynamic assays.

Some general comments can be made concerning the current state-of-the-art for using procedure 1 to enhance thermal stability of poling-induced second order optical nonlinearity. Currently, stability for periods of several thousand hours at temperatures in the range 90 to 150°C are realized with this approach. This is by no means the ultimate stability possible with this approach since complete lattice hardening has not likely been realized and the polymers currently used contain extended flexible chain segments. Reduction of the extent of flexible chain segments should permit long term stability at higher temperatures to be realized; however, this improvement may be at the price of some reduction in poling efficiency. Employing azobenzene chromophores, we have achieved thermally stable r_{33} values in the range 7-13 pm/V (using a sulfonyl acceptor) and 14-20 pm/V (using a nitro group acceptor) [24a]. Waveguides with optical losses, at 1.3 micron wavelength, on the order of 0.1 dB/cm have been fabricated from these materials. With high β chromophores, thermally-stable electro-optic coefficient values of 30 pm/V have been achieved although it should be noted that these values do not reflect the optimization of poling protocols for these

materials. Representative syntheses of polymer lattices incorporating high $\mu\beta$ chromophores are shown in Figs. 9 and 10.

Two general synthetic approaches have been employed to achieve modified polyimide lattices containing covalently incorporated chromophores. These schemes are illustrated in Fig. 11 and representative data on the thermal stability of NLO activity is shown in Fig. 12. The behavior observed for these modified polyimide systems is similar to that observed for the lattices prepared by procedure 1. Electro-optic coefficients are slightly less and the thermal stability is slightly superior (long term stability has been observed to temperatures as high as 175°C). The processing protocol is similar between procedures 1 and 2 in that in both cases a processible precursor (to the final hardened polymer) polymer is prepared. In procedure 2, the processible material is a polyamic acid. A problem with the imidization step is that quite high temperatures are required for complete imidization. If these temperatures are not achieved in the hardening step, then lattice condensation may occur during thermal aging at elevated temperatures. We typically observed this phenomena as a slow loss of optical nonlinearity with aging. Another feature of modified polyimides worth noting is that, depending upon the exact nature of the structure, it may be difficult to achieve films of high optical quality. This is likely due to the fact that spin casting options (e.g., choice of solvent) are more limited for modified polyamic acids than for the precursor polymers of procedure 1.

Two different schemes following procedure 3 are illustrated in Figs. 13 and 14 and representative thermal stability data is shown in Fig. 15. Again, in the broader sense, comparable thermal stability and optical nonlinearities are observed for this approach as for procedures 1 and 2. At a closer level of comparison the magnitudes of the electro-optic coefficients and the thermal stability of nonlinear optical activity are not quite as good with this approach; this observation likely reflects the fact that the poling and lattice hardening steps are not cleanly separated and the latter interferes with the former. Moreover, complete lattice hardening is realized only at elevated temperatures so that temporal stability studies often reveal a slow evolution of optical nonlinearity. Of course, an advantage of procedure 3 is that it permits modified sol-gel glasses to be prepared which may be of potential utility for interfacing with fiber optic transmission lines.

At this point in time no absolute preference can be argued for one of the above three procedures although prototype devices have largely been fabricated employing procedures 1 and 2. Clearly, more effort is required to optimize and evaluate each of the approaches. On the positive side, it is already clear that any of the above approaches can fulfill the thermal requirements for some electro-optic modulator applications.

The importance of electric field poling protocol should be evident from a consideration of the above procedures and particularly for procedure 3. Using corona poling, we frequently employ protocols which involve different sequences of stepped increases in poling field and temperature. Various protocols are explored to optimize $\langle\cos^3\theta\rangle$. Of course, materials must be free of ionic and dipolar impurities to avoid breakdown and ionic conductivity as the poling field is increased. Optimum poling leads to a stable maximum of optical nonlinearity with poling voltage.

A number of research groups are beginning the much needed detailed study of poling (e.g., distribution of space charge) and subsequent relaxation of charge and of molecular order in poled polymers [27].

A variety of additional schemes for realizing hardened lattices, including the development of interpenetrating polymer networks by Tripathy [28], have also been pursued. In addition to the literature already cited, the reader is referred to a recent review by Burland, Miller, and Walsh [29].

4.3 Preparation of buried channel nonlinear optical waveguides

Four different procedures have been utilized for the fabrication of buried channel nonlinear optical waveguides [10,20,30]. These include (1) photochemical processing [10,20,30], (2) reactive ion etching (RIE) [10,20,30e], (3) laser etching [10,20], and (4) spatially selective poling [10].

A variety of photochemical processes can lead to reduction in index of refraction or change in birefringence necessary to prepare a channel waveguide structure [10]. These include trans-to-cis isomerizations (such as encountered with azobenzene chromophores), ring opening reactions, photo-induced keto-enol tautomerism, interconversion between charge transfer conformations, polymerization reactions, etc. Most of the photochemical processing reported in the literature, including the work carried out at USC, has focused upon trans-to-cis isomerization [10]. Note that the actual mechanism of index change observed for azobenzenes is more complex than simple trans-to-cis isomerization and likely involves rapid relaxation back to the trans conformation but in such a manner that the net effect is that of molecular reorientation.

Photochemical processing can be used to fabricate a buried channel waveguide directly without deposition of a cladding layer. The procedure involves two step, two color processing with change of the mask between steps. The development of a buried channel by this procedure depends upon the fact that the penetration of the radiation into the sample will depend upon radiation wavelength. The first step involves use of a mask to protect a channel of high index, nonlinear optical material from the top of the film to the bottom. Radiation at a wavelength characterized by low absorption (hence good penetration through the film) is used to reduce the index of refraction of the material around the protected region. The low absorption must, of course, be offset by a long exposure time to achieve effective bleaching. Following this step, the mask is removed and the unbleached region is exposed to radiation of a wavelength corresponding to (or closer to) the absorption maximum. Electromagnetic radiation of such a wavelength has a shallow penetration depth so bleaches only the uppermost region creating a buried channel of unbleached, nonlinear optical material. Moving from the bottom to the top of the material (Fig. 16a), one finds (1) the lower cladding layer, (2) the unbleached, high index, nonlinear optically active channel, and (3) the bleached, low index upper layer. Thus, a buried channel of nonlinear optical material (waveguide) has been effected without deposition of an upper cladding layer.

A serious problem in system integration is that of coupling the rather small (e.g., 1 to 3 micron) waveguide of an electro-optic modulator to the large waveguide structure of a fiber optic transmission line. One approach to this procedure is to develop a tapered waveguide structure progressing from a few microns to approximately 8-10 microns. (Other approahes include control of both depth and width of the waveguide to ensure single mode operation while achieving adequate mode overlap and the use of a focusing lens to optimize coupling.) However, large waveguide dimensions pose problems for single mode operation. Let us briefly review the criteria for single mode guiding.

For single mode operation, local gradients, if large, must be sufficiently small in size (0.5-1.5 μm for refractive index differences between 0.5 and 1.5). This is fine for small device dimensions, but leads to a gross mismatch with the larger mode sizes of optical fibers because these have small, graded index (small Δn) cores. This mismatch has been a persistent problem to device development with NLO polymer materials because unless polymer claddings are closely matched in index, single mode operation requires small waveguide dimensions which mismatch fiber mode sizes. Early innovations to make thick

films with small Δn claddings and boundaries (0.01-0.03 for 10 μm waveguide dimensions) for channel waveguides led to innovations in specialized claddings such as NLO polymer blends, e.g., the HCC 1232-1232A polymers developed in the late 1980's by Hoechst Celanese [31]. A number of methods for creating large single mode (small Δn) waveguides have been developed including reactive ion etching (RIE) of ribs in small Δn claddings [30e,32], and induced birefringence in small Δn claddings [33].

An inherent shortcoming of all approaches to make large single-mode waveguides in thin films stems directly from the need for small Δn boundaries. This necessitates thick cladding layers because large single modes are strongly evanescent in small Δn claddings; however, thick claddings result in low device sensitivity because of large electrode spacings. Moreover, serious fabrication difficulties (cracking of film laminates, solvent damage, and other stress-related problems) are encountered with thick claddings.

The multi-color photolithography technique mentioned above is ideally suited for processing buried channel (small Δn) waveguides without the requirement of cladding layers. Small Δn gradients can be realized by exploiting the known penetration profiles of electromagnetic radiation of various wavelengths into the photoactive polymer material. The tapered transition shown in Fig. 1c which can be effected by a combination of photochemical processing and reactive ion etching provides a particularly attractive route to satisfying the requirements for single mode guiding, good coupling efficiency, and high modulator efficiency.

To accomplish the precise index control discussed above, one must be able to model the photochemical processing (dynamics) with high accuracy. Photochemical modeling appears to be well in hand for azobenzene and stilbene type chromophores [10,20,30,34].

The second method that we have employed to fabricate buried channel waveguides is reactive ion etching and the general scheme is outlined in Fig. 17. An oxygen plasma is known to react with most organic polymers. This method does not change the refractive index but rather the shape of the thin films as indicated in Fig. 17. Most waveguides prepared with RIE have a ridge cross section so the waveguide area is protected and the surrounding area is exposed to an oxygen plasma. In our experiments, we typically coat a layer of photoresist (Shipley 1400-17) directly on to the surface of a poled polymer film so that an etch mask can be defined to protect the desired waveguide region. We use a mask aligner and a laser patterned photomask in our photolithographic process. The etch mask is obtained after development and rinse with deionized water. The structure is then etched in a Plasma Technology model DP80M RIE apparatus employing 200 millitorr oxygen pressure and 100 watts radiofrequency power. For a typical azobenzene containing polymer such as discussed above, the initial etch rate was approximately sixty angstroms/second while the etch rate of the photoresist was on the order of approximately twenty angstroms/second. An advantage of the RIE method is that it is compatible with silicon v-groove technology for the pigtailing of the nonlinear optical channel to fiber optic transmission lines. Moreover, the RIE method can be more generally applied than photochemical processing in that it does not require the presence of a photoactive species. Finally, we note that RIE avoids the problem of unwanted photochemical aging of structures with exposure to environmental radiation during the lifetime of the device. However, we emphasize that it is clearly possible to use more than one technique in processing a material for nonlinear optical applications and it is possible to encapsulate materials to avoid environmental radiation; thus, a discussion of the advantages of one method versus another is somewhat misleading. To make this point more explicit we show a schematic representation in Fig. 1c of an optical switching node in a cable

network which is fabricated by a combination of multi-color photochemical processing and reactive ion etching techniques.

As discussed above, index of refraction variations and the dimensions of the buried channel structure define mode propagation characteristics of the waveguide. Single mode propagation is desired in many devices such as integrated Mach-Zehnder interferometers. Since the indices of the films are fixed and not easily varied (except by photochemical processing as discussed above), we choose two parameters, film thickness and etching depth, to control modal characteristics when using RIE. From the standpoint of optical fiber coupling, we desire to maximize the waveguide cross section to reduce coupling losses. Thus, we first calculate the maximum film thickness using the effective index method, to determine the maximum waveguide width at a given etch depth and maximum film thickness for single mode operation. The dimensional requirements for single mode operation in our polyimide polymer of Fig. 11b are shown in Fig. 17b. This approach optimizes modulator waveguide/fiber mode overlap without resorting to the tapered transition of Fig. 1c; thus, photochemical processing is avoided.

Laser etching is analogous to RIE but uses laser ablation to define the ridge or channel. Care must be taken in this process to insure that the active region temperature does not exceed the depoling temperature of the polymer or alternately the poling must be poled after the laser etch process.

Spatially selective poling produces a birefringence of aligned poled material. This approach suffers from the disadvantage of limiting poling configuration so that corona and in-plane configurations are not conveniently used. The result is often some reduction in poling efficiency.

4.1 Integration of NLO waveguides into circuits, devices, and networks

A schematic representation of a representative electro-optic modulator and associated test bed is shown in Fig. 18. It is clear that once a buried channel nonlinear optical waveguide has been fabricated these components must be integrated with the remaining optical and electronic circuitry.

Optical integration has been accomplished either by prism coupling or by pigtailing to fiber optic transmission lines. Prism coupling is convenient and has been the most commonly used approach. However, this mode of coupling is not commercially viable and is of utility only for prototype device demonstration. Commercial applications of electro-optic modulators require a compact, efficient, and mechanically stable coupling to commercially available fiber optic transmission lines. Pigtailing to fiber optic lines appears to be a critical area for the development of practical electro-optic modulators. The have chosen to effect pigtailing by exploiting silicon v-groove technology. A typical coupling scheme is shown in Fig. 19. A meaningful evaluation of the ultimate coupling efficiency which can be realized by this approach cannot be given at this time. Indeed, a great deal remains to be done to optimize coupling efficiency, e.g., photochemical tuning of indices of refraction to achieve optimum coupling as discussed above. However, this technique works sufficiently well at this time to permit construction and evaluation of prototype devices.

Deposition of metal electrodes and optimization of the coupling of radiofrequency (microwave, millimeter wave) radiation into the nonlinear optical waveguides is again a process which can be reasonably well accomplished with current materials but is an area where improvements can be carried out by improved electrode design, by development of improved materials, and by development of creative processing techniques.

As most modulators have been fabricated in a Mach-Zehnder configuration, let us, in this discussion, illustrate the birefringence modulator which can be used either as a phase or a birefringence amplitude modulator. If the input is either a pure TE or a pure TM mode, the device acts as a phase modulator. If the input beam excites both TE and TM modes, the birefringence of the waveguide is changed by the applied voltage and the output polarization changes according to the modulation field. The analyzer shown in Fig. 1b converts the polarization modulation into an amplitude modulation. Representative modulation signals are shown in Fig 20. These signals were detected using an InGaAs p-i-n photodetector (Fermionics FD80S) and monitored by a Hewlett-Packard HP8652A spectrum analyzer or displayed directly on an oscilloscope (for low frequecny modulation). Although these signals were obtained using thick cladding layers (total device thickness approximately 15 microns) and the modulator uses only 2/3 of the available r_{33} nonlinearity, a half-wave V_π voltage of 35 volts was obtained using a 15 mm electrode (this corresponds to an electro-optic coefficient of 12 pm/V which was expected for the azobenzene incorporated polymer used).

For the sake of completeness, it is appropriate to review the fabrication of the modulator used to obtain the data shown in Fig. 20. The nonlinear optical material is an azobenzene containing polyurethane processed according to procedure 3. Fused quartz slides (ESCO products, Inc.) were used as substrate materials. A layer of gold (approximately 0.5 micron thick) was sputtered using an argon plasma sputtering system. The lower and upper polymer claddings were cast from commercial polyurethane (Epoxylite 9653-1). The lower cladding was first spin-cast on the gold coated substrate as was baked at 90°C for several hours. The NLO material was dissolved in dioxane and was spin cast into approximately one micron films using a spin speed of approximately 1000 rpm. The film was then heated and poled using a corona discharge set-up with needle to plane distance of approximately 2 cm. A 5.5 KV voltage was applied. The temperature was raised to approximately 160°C and the hardening reaction initiated. The NLO waveguide was then defined by RIE as discussed above. The top cladding layer was spun on top of the etched surface and was cured at room temperature. The upper electrode with dimensions of 15 mm length and 30 microns width was defined photolithographically and was plated to 5 micron thickness to reduce DC resistance.

Both Mach-Zehnder and birefringent modulator designs have been evaluated to frequencies approaching 40 GHz and require V_π voltages in the range 10-50 volts (depending on the chromophore used, cladding layer thickness, processing conditions, electrode design, etc.) [35]. Performance at wavelengths from 0.83 to 1.3 microns has been evaluated. Commercial application will require further improvement in V_π, namely, reduction of required drive voltages to digital voltage levels. A critical area of focus for the realistic achievement of modulation at frequencies above 50 GHz is electrode design as losses at electrodes appear to be the limiting factor in the frequency range 50-100 GHz.

An important area of activity which deserves more attention is that of improved device design. This aspect is illustrated by a recent paper by Garito and coworkers which presents an improved design for a directional coupler [36].

5 Concluding remarks

Considerable expectations have been raised for a new era of communication technology based upon new materials and new phenomena. It is probably important for scientist to keep in mind that financial realities (e.g., availability of investment capital) may have a greater impact upon realization of new technologies than scientific issues. While potential markets, such as the cable television industry and the government, can be identified

it is difficult to ascertain how motivated these markets will be to incorporate new materials technologies in times of depressed economies. Moreover, in this brief review, we have not had time to address all related technologies, e.g., information handling software; and it is a hard reality that all relevant technologies and an attractive financial climate must be available for effective implementation of a new technology.

What we have been able to do in this brief review is to provide some brief insight into materials issues and the competitiveness of various classes of materials. Currently, available organic (polymeric) and inorganic (crystalline) materials appear to be comparable in terms of electro-optic coefficients (modulation efficiencies) while organic materials, due to their small dielectric constants, offer significant advantages in terms of bandwidths. (However, the need for bandwidths greater than 10 GHz is not, in general, a serious market issue at this time.) Where inorganic materials appear to have a significant advantage is the level of engineering effort that has been expended to integrate these into operational systems. In this review, we have hopefully shown that organic (polymeric) materials can be effectively integrated in systems and indeed may afford a number of significant advantages relative to inorganic materials such as lithium niobate for systems integration. These advantages include ease of integration, cost, and the ability to transition to fiber optic lines with low loss, mechanically stable couplings which can be fabricated with well-defined RIE and photolithographic techniques. It should be clear from our review that modulation efficiency in organic materials is determined by the hyperpolarizability of the chromophore employed, number density of the chromophore in the polymer matrix, and by the poling-induced order. It is unlikely that the state of the art for realization of chromophore incorporation or ordering will be improved upon; however, high hyperpolarizability chromophores have been identified and if these can be incorporated in high density and poled with good efficiency then it should be possible to significant exceed the modulation efficiencies of inorganic materials. If both superior modulation efficiencies and system integration capabilities with organic materials are realized, it is clear that they have the potential to compete with inorganic materials if significant markets develop.

This review has been focused upon the research activities most relevant to commercialization. This seems appropriate since potential technological relevance is clearly a factor motivating interest in nonlinear optical materials. However, we emphasize that several areas of great interest from a fundamental scientific view have been explored in the study of nonlinear optical materials. These include development of ultrastructures (or nanoscale structures) by techniques of sequential synthesis and molecular self-assembly. Critical fundamental studies are also being effected on the dynamics of induction and relaxation of molecular order by electric field poling. Development of a body of knowledge in these fundamental areas could prove invaluable to realizing a significant breakthrough in preparation of materials for device applications.

References

[1] *D. Hilliard and D. Mensa*: Proc. IEEE Antenna and Prop. Soc. Symp. **2** (1992) 720.

[2] *M. Segev, G. Duree, G. Salamo, B. Crosignani, P. DiPorto, A. Yariv, E. Sharp, and R. Neurgaonkar*: in Proc. Quant. Elect. and Laser Sci. Conf., OSA Technical Digest Series (1994) in press.

[3] (a) *M. E. Orczyk, J. W. Zieba, and P. N. Prasad*: Proc. SPIE **2025** (1993) 298.
(b) *Y. Zhang, Y. Cui, and P. N. Prasad*: Phys. Rev. B **46** (1992) 9900.
(c) *C. A. Walsh and W. E. Moerner*: J. Opt. Soc. Am. B **9** (1992) 1642.
(d) *W. E. Moerner, C. Walsh, J. C. Scott, S. Ducharme, D. M. Burland, G. C. Bjorklund, and R. J. Twieg*: Proc. SPIE **1560** (1991) 278.
(e) *S. Ducharme, J. C. Scott, R. J. Twieg, and W. E. Moerner*: Phys. Rev. Lett. **66** (1991)1846.
(f) *J. S. Schildkraut*: Appl. Phys. Lett., **58** (1991) 340.
(g) *M. J. Sansone, C. C. Teng, A. J. East, and M. S. Kwiatek*: Proc. SPIE **2025** (1993) 277.
(h) *B. Kippelen, Sandalphon, K. Meerholz, B. Volodin, S. R. Lyon, A. B. Padias, H. K. Hall, Jr., and N. Peyghambarian*: Proc. Mat. Res. Soc. **328** (1994) 577.
(i) *W. E. Moerner and S. M. Silence*: Chem. Rev. **94** (1994) 127.

[4] (a) *L. P. Yu, W. K. Chan, Y. Chen, and Z. Peng*: in Proc. Mat. Res. Soc. **328** (1994) 63.
(b) *L. P. Yu, W. Chan, Y. Chen, Z. Peng, Z. Bao, and D. Yu*: Proc. SPIE **2025** (1993) 268.
(c) *H. J. Bolink, V. V. Krasnikov, G. G. Malliaras, and G. Hadzioannou*: Proc.SPIE **2025** (1993) 292.

[5] *J. W. Perry, S. R. Marder, K. J. Perry and E. T. Sleva*: Proc. SPIE **1560** (1991) 302.

[6] (a) *D. C. Rodenberger, J. R. Heffin, and A. F. Garito*: Nature **359** (1992) 309.
(b) *L. R. Dalton*: Nature **359** (1992) 269.

[7] (a) *J. Zyss*: Nonlinear Opt. **1** (1991) 3.
(b) *J. Zyss and I. Ledoux*: Chem. Rev. **94** (1994) 77.
(c) *B. M. Pierce, J. Zyss, and M. Joffre*: Proc. SPIE **2025** (1993) 3.
(d) *T. Verbiest, K. Clays, A. Persoons, C. Samyn, F. Meyers, and J.-L. Bredas*: Proc. SPIE **2025** (1993) 31.

[8] (a) *D. R. Kanis, M. A. Ratner, and T. J. Marks*: Chem. Rev. **94** (1994) 195.
(b) *J. L. Bredas, C. Adant, P. Tackx, A. Persoons, and B. M. Pierce:* Chem. Rev. **94** (1994) 243.

[9] (a) *S. R. Marder and J. W. Perry*: Science **263** (1994) 1706 and references cited therein.
(b) *S. R. Marder, D. N. Beratan, and L.-T. Cheng*: Science **252** (1991) 103.
(c) *C. B. Gorman and S. R. Marder*: Proc. Natl. Acad. Sci. USA **90** (1993) 11297.
(d) *G. Bourhill, L.-T. Chang, G. Lee, S. R. Marder, J. W. Perry, M. J. Perry, and B. G. Tiemann*: Proc. Mat. Res. Soc. **328** (1994) 625 and references contained therein.
(e) *D. R. Kanis, M. A. Ratner, and T. J. Marks*: Chem. Rev. **94** (1994) 195.
(f) *J. L. Bredas, C. Adant, P. Tackx, and A. Persoons*: Chem. Rev. **94** (1994) 243.

[10] *L. R. Dalton, L. S. Sapochak, M. Chen, and L. P. Yu*: Ultrastructure Concepts of Optical Integrated Microcircuits and Polymeric Materials. In: *K. Sienicki* (ed.) "Molecular Electronics and Molecular Electronic Devices". Vol. 2, 125. CRC Press, Boca Raton, 1993 and references contained therein.

[11] (a) *S. Yamada, Y. M. Cai, R. F. Shi, M. H. Wu, W. D. Chen, Q. M. Qian, and A. F. Garito*: Proc. Mat. Res. Soc. **328** (1994) 523.
(b) *R. J. Twieg, D. M. Burland, J. L. Hedrick, V. Y. Lee, R. D. Miller, C. R. Moylan, W. Volksen, and C. A. Walsh*: Proc. Mat. Res. Soc. **328** (1994) 421.
(c) *R. J. Twieg, K. M. Betterton, D. M. Burland, V. Y. Lee, R. D. Miller, C. R. Moylan, W. Volksen, and C. A. Walsh*: Proc. SPIE **2025** (1993) 94.
[12] (a) *K. Y. Wong and A. K.-Y. Jen*: J. Appl. Phys. in press.
(b) *A. K.-Y. Jen, V. P. Rao, K. J. Drost, Y. M. Cai, R. M. Mininni, J. T. Kenney, E. S. Binkley, L. R. Dalton, and S. R. Marder*: Proc. SPIE **2143** (1994) in press.
(c) *A. K.-Y. Jen, K. Drost, V. P. Rao, Y. M. Cai, R. M. Mininni, J. Kenney, E. Binkley, L. R. Dalton, and C. Xu*: J. Opt. Soc. Amer. B in press.
[13] (a) *R. F. Shi, M. H. Wu, S. Yamada,Y. M. Cai, and A. F. Garito*: Appl. Phys. Lett. **63** (1993) 1173.
(b) *M. R. McLean, M. Badr, L. R. Dalton, R. L. S. Devine, and W. H. Steier*: J. Phys. Chem. **94** (1990) 4386.
[14] *F. London*: Trans. Faraday Soc. **33** (1937) 8.
[15] (a) *D. S. Chemla and J. Zyss* (eds.): Nonlinear Optical Properties of Organic Molecules and Crystals. Academic Press, New York, 1987.
(b) *P. N. Prasad and D. J. Williams*: Introduction to Nonlinear Optical Effects in Molecules and Polymers. John Wiley & Sons, New York, 1991.
(c)*P. J. Halfpenny, E. E. A. Shepherd, J. N. Sherwood, and G. S. Simpson*: Proc. SPIE **2025** (1993) 171.
(d) *M. Zaworotko, S. Subramanian, and L. R. MacGillivray*: Proc. Mat. Res. Soc. **328** (1994) 107.
(e) *P. G. Lacroix, R. Clement, K. Nakatani, I. Ledoux, and J. Zyss*: Proc. Mat. Res. Soc. **328** (1994) 613.
(f) *G. Wegner, D. Neher, C. Heldmann, Th. K. Servay, H.-J. Winkelhahn, M. Schulze, and C.-S. Kang*: Proc. Mat. Res. Soc. **328** (1994) 15.
[16] (a) *G. Decher, B. Tieke, Ch. Bosshard, and P. Gunter*: Ferroelectrics **91** (1989) 193.
(b)*T L.Penner, N. J. Armstrong, C. S. Willand, J. S. Schildkraut, and D. R. Rebello*: Proc. SPIE **1560** (1991) 377.
(c)*A. Ulman*: An Introduction to Ultrathin Organic Films: From Langmuir-Blodgett to Self-Assembly. Academic Press, New York 1991.
(d) *N. Asai, I. Fujiwara, H. Tamada, and J. Seto*: Proc. Mat. Res. Soc. **328** (1994) 91.
(e) *A. C. Fou, D. L. Ellis, and M. F. Rubner*: Proc. Mat. Res. Soc. **328** (1994) 113.
[17] (a) *S. Yitzchaik, A. K. Kakkar, S. B. Roscoe, T. J. Marks, P. M. Lundquist, W. Lin and G. K. Wong*: Proc. Mat. Res. Soc. **328** (1994) 27.
(b) *S. Yitzchaik, S. B. Roscoe, A. K. Kakkar, D. S. Allan, T. J. Marks, Z. Xu, T. Zhang, W. Lin, and G. K. Wong*: J. Phys. Chem. **97** (1993) 6958.
(c) *A. K. Kakkar, S. Yitzchaik, S. B. Roscoe, F. Kubota, D. S. Allan, T. J. Marks, W. Lin, and G. K. Wong*: Langmuir **9** (1993) 388.
(d) *D. Li, M. A. Ratner, T. J. Marks, C. Zhang, J. Yang, and G. K. Wong*: J. Am. Chem. Soc. **112** (1990) 7389.
(e) *L. R. Dalton, C. Xu, B. Wu, and A. W. Harper*: Techniques for Ultrastructure Synthesis: Preparation of Second Order Nonlinear Optical Materials. In: *P.N. Prasad* (ed.) "Proc. 2nd. Int. Conf. on Frontiers of Polymers and Adv. Materials". 175, Plenum, New York 1994.
[18] (a) *H. E. Katz, M. L. Schilling, S. Ungashe, T. M. Putvinski, G. Scheller, C. E. D. Chidsey, and W. L. Wilson*: Proc. SPIE **1560** (1991) 370.

(b) *H. E. Katz, G. Scheller, T. M. Putvinski, M. L. Schilling, W. L. Wilson, and C. E. D. Chidsey*: Science **254** (1991) 1486.
(c) *G. Cao, H. Hong, and T. E. Mallouk*: Accts. Chem. Res. **25** (1992) 420.
(d) *S. D. Ungashe, W. L. Wilson, H. E. Katz, G. Scheller, and T. M. Putvinski*: J. Am. Chem. Soc. **114** (1992) 8718.
(e) *H. E. Katz, S. F. Shane, W. L. Wilson, M. L. Schilling, and S. B. Ungashe*: Proc. Mat. Res. Soc. **328** (1994) 361.
[19] (a) *J. F. Lam, S. R. Forrest, and G. L. Tangonan*: Phys. Rev. Lett. **66** (1991) 1614.
(b) *F. F. So and S. R. Forrest*: Phys. Rev. Lett. **66** (1991) 2629.
(c) *S. R. Forrest, P. E. Burrows, E. I. Haskal, and Y. Zhang*: Proc. Mat. Res. Soc. **328** (1994) 37 and references cited therein.
(d) *T. Wada, M. Hosoda, A. F. Garito, H. Sasabe, A. Terasaki, T. Kobayashi, H. Tada, and A. Koma*: Proc. SPIE **1560** (1991) 162.
[20] (a) *L. R. Dalton, C. Xu, A. W. Harper, R. Ghosn, B. Wu, Z. Liang, R. Montgomery, and A. K.-Y. Jen*: Nonlinear Opt. in press.
(b) *L. R. Dalton, B. Wu, A. W. Harper, Z. Liang, R. Ghosn, J. Laquindanum, C. Xu, W. H. Steier, A. K.-Y. Jen, R. Mustacich, and H. Fetterman*: Chemistry of Materials, submitted.
[21] (a)*M. B. Meinhardt, P. A. Cahill, C. H. Seager, A. J. Beuhler, and D. A. Wargowski*: Proc. Mat. Res. Soc. **328** (1994) 467.
(b) *P. A. Cahill, C. H. Seager, M. B. Meinhardt, A. J. Beuhler, D. A. Wargowski, K. D. Singer, T. C. Kowalczyk, and T. Z. Kose*: Proc. SPIE **2025** (1993) 48.
[22] (a) *H. H. Fujimoto, S. Das, J. F. Valley, M. Stiller, L. Dries, D. Girton, T. Van Eck, S. Ermer, E. S. Binkley, J. C. Nurse, and J. T. Kenney*: Proc. Mat. Res. Soc. **328** (1994) 553.
(b) *J. Wu, J. F. Valley, S. Ermer, E. S. Binkley, J. T. Kenney, G. F. Lipscomb, and R. Lytel*: Appl. Phys. Lett. **58** (1991) 225.
(c) *J. F. Valley, J. W. Wu, S. Ermer, M. Stiller, E. S. Binkley, J. T. Kenney, G. F. Lipscomb, and R. Lytel*: Appl. Phys. Lett. **60** (1992) 160.
[23] (a) *M. A. Hubbard, N. Minami, C. Ye, T. J. Marks, J. Ynag, and G. K. Wong*: Proc. SPIE **971** (1988) 136.
(b) *M. A. Hubbard, T. J. Marks, J.Yang, and G. K. Wong*: Chem. Mater. **1** (1989) 167.
(c) *J. Parks, T. J. Marks, J. Yang, and G. K. Wong:* Chem. Mater. **2** (1990) 229.
(d) *Y. Jin, S. H. Carr, T. J. Marks, W. Lin, and G. K. Wong:* Chem. Mater. **4** (1992) 963.
(e) *M. Eich, B. Reck, C. G. Wilson, D.Y. Yoon, and G. C. Blorklund*: J. Appl. Phys. **66** (1989) 3241.
[24] (a) *C. Xu, B. Wu, L. R. Dalton, Y. Shi, P. M. Ranon, S. Kalluri, and W. H. Steier*: Proc. Mat. Res. Soc. **328** (1994) 461.
(b) *B. Wu, C. Xu, L. R. Dalton, S. Kalluri, Y. Shi, and W. H. Steier*: Proc. Mat. Res. Soc. **328** (1994) 529.
(c) *J.-F. Wang, M. A. Hubbard, Y. Jin, J. T. Lin, T. J. Marks, W. P. Lin, and G. K. Wong*: Proc. SPIE **2025** (1994) 62.
(d) *M. Eich, M. Ohl, R. Zentel, and W. Schulz-Hanke*: Proc. SPIE **2025** (1993) 78.
(e) *C. Xu, M. W. Becker, B. Wu, L. R. Dalton, Y. Shi, P. M. Ranon, and W. H. Steier*: Proc. SPIE **2025** (1994) 21 and reference contained therein.
(f) *J. D. Strenger-Smith, J. W. Fischer, R. A. Henry, J. M. Hoover, G. A. Lindsay, and L. M. Hayden*: Makromol. Chem., Rapid Commun. **11** (1990) 141.
(g) *F. Fuso, A. B. Padias, and H. K. Hall, Jr.*: Macromolecues **24** (1991) 1710.
[25] (a) *M. A. Hubbard, T. J. Marks, W. Lin, and G. K. Wong*: Chem. Mater. **4** (1992) 965.

(b) *B. Zysset, M. Ahlheim, M. Stahelin, F. Lehr, P. Pretre, P. Saatz, and P. Gunter:* Proc. SPIE **2025** (1993) 70.

(c) *M. W. Becker, L. S. Sapochak, L. R. Dalton, Y. Shi, W. H. Steier, and A. K. Jen:* Chem. Mater. **6** (1994) 104.

(d) *A. K.-Y. Jen, K. J. Drost, Y. Cai, V. P. Rao, and L. R. Dalton:* J. Chem. Soc., Chem. Commun. (1994) 965.

(e) *A. K.-Y. Jen, V. P. Rao, K. J. Drost, Y. M. Cai, R. M. Mininni, J. T. Kenney, E. S. Binkley*, L. R. Dalton, and S. R. Marder: Chem. Mater. in press.

(f) *S.Yang, Z. Peng, and L. P. Yu:* Macromolecules in press.

(g) *J. T. Lon, M. A. Hubbard, T. J. Marks, W. Lin, and G. K. Wong:* Chem. Mater. **4** (1992) 1148.

[26] (a) *M. Chen, L. R. Dalton, L. P. Yu, Y. Shi, and W. H. Steier:* Macromolecules **25** (1992) 4032.

(b) *M. Chen, L. P. Yu, L. R. Dalton, Y. Shi, and W. H. Steier:* Macromolecules **24** (1991) 5421.

(c) *C. V. Francis, K. M. White, G. T. Boyd, R. S. Moshrefzadeh, S. K. Mohapatra, M. D. Radcliffe, J. E. Trend, and R. C. Williams*: Chem. Mater. **5** (1993) 506.

(d) *R. J. Peng, Y. M. Chen, a. K. Jain, J. Kumar, and S. K. Tripathy:* Chem. Mater. **4** (1992) 972.

(e) *J. Kim, J. L. Plawsky, R. LaPeruta, and G. M. Korenowski*: Chem. Mater. **4** (1992) 249.

(f) *J. Kim, J. L. Plawsky, E. Van Wagenen, and G. M. Korenowski*: Chem. Mater. **5** (1993) 1118.

(g) *J. B. Caldwell, R. W. Cruse, K.J. Drost, V. P. Rao, A. K.-Y. Jen, K. Y. Wong, Y. M. Cai, R. M. Mininni, J. Kenney, E. Binkley, L. R. Dalton, Y. Shi, and W. H. Steier:* Proc. Mat. Res. Soc. **328** (1994) 535.

[27] (a) *K. S. Haber, M. H. Ostrowski, M. J. O'Sickey, and H. S. Lackritz:* Proc. Mat. Res. Soc. **328** (1994) 595.

(b) *K. D. Singer, R. Dureiko, J. Khaydarov, and R. Fuerst*: Proc. Mat. Res. Soc. **328** (1994) 499.

(c) *A. Dhinojwala, J. C. Hooker, and J. M. Torkelson*: Proc. Mat. Res. Soc. **328** (1994) 443.

(d) *R. Meyrueix, G. Tapolsky, M. Dickens and J.-P. Lecomte*: Proc. SPIE **2025** (1993) 117.

(e) *D. M. Burland, R. D. Miller, and C. A. Walsh*: Chem. Rev. **94** (1994) 31.

[28] (a) S. *Marturunkakul, J.-I. Chen, L. Li, X. L. Jiang, R. J. Jeng, J. Kumar, and S. K. Tripathy*: Proc. Mat. Res. Soc. **328** (1994) 541.

[29] *D. M. Burland, R. D. Miller, and C. A. Walsh* : Chem. Rev. **94** (1994) 31.

[30] (a) *Y. Shi, W. H. Steier, L. Yu, M. Chen, and L. R. Dalton*: Appl. Phys. Lett. **58** (1991) 1131.

(b) *Y. Shi, W. H. Steier, L. Yu, M. Chen, and L. R. Dalton:* Appl. Phys. Lett. **59** (1991) 2935.

(c) *W. H. Steier, Y. Shi, L. P. Yu, M. Chen, and L. R. Dalton*: Proc. SPIE **1775** (1992) 379.

(d) *Y. Shi, P. M. Ranon, W. H. Steier, C. Xu, B. Wu, and L. R. Dalton:* Proc. SPIE **2025** (1993) 106.

(e) *W. H. Steier, Y. Shi, P. M. Ranon, C. Xu, B. Wu, L. R. Dalton, W. Wang, D. Chen, and H. Fetterman:* Proc SPIE **2025** (1993) 535.

(f) *K. W. Beeson, K. A. Horn, M. J. McFarland, and J. T. Yardley:* Appl. Phys. Lett. **58** (1991) 1955.
(g) *K. W. Beeson, M. J. McFarland, W. A. Pender, J. Shan, C. Wu, and J. T. Yardley:* Proc. SPIE **1794** (1993) 397.
(h) *M. J. McFarland, K. W. Beeson, K. A. Horn, A. Nahata, C. Wu, and J. T. Yardley:* Proc. SPIE **1583** (1991) 344.
(i) *K. W. Beeson, K. A. Horn, C. Lau, M. J. McFarland, D. Schwind, and J. T. Yardley:* Proc. SPIE **1559** (1991) 258.
(j) *K. W. Beeson, K. A. Horn, M. J. McFarland, A. Hahata, C. Wu, and J. T. Yardley:* Proc. SPIE **1337** (1990) 195.
(k) *K. W. Beeson, K. A. Horn, M. J. McFarland, C. Wu, and J. T. Yardley:* Proc. SPIE **1374** (1991) 176.
(l) *R. Srinivasan:* J. Appl. Phys. **72** (1992) 1651.
(m) *R. Srinivasan:* Appl. Phys. Lett. **58** (1991) 2895.
(n) *R. Srinivasan and B. Braren:* Appl. Phys. A **45** (1988) 289.
(o) *M. Ritz, V. Srinivasan, S. V. Babu, and R. C. Patel:* Proc. Mat. Res. Soc. **75** (1987) 433.
[31] *H. T. Man, K. Chiang, D. Haas, C. C. Teng, and H. N. Yoon:* Proc. SPIE **1213** (1990) 7.
[32] *C. C. Teng, D. R. Haas, H. T. Man, and H. N. Yoon:* in "Integrated and Guided-Wave Optics", Technical Digest Series, 5. Optical Society of America, Washington, D.C. 1988, 377.
[33] (a) *R. Mustacich, M. Gilbert, R. Finn, and C. Swann:* Appl. Opt. **31** (1992) 2800.
(b) *R. Mustacich:* Appl. Opt. **27** (1988) 3732.
[34] (a) *F. H. Dill, W. P. Hornberger, P. S. Hauge, and J. M. Shaw:* IEEE Trans. Electr. Dev. ED **22** (1975) 445.
(b) *D. Dantsker and S. Speiser:* Proc. SPIE **2025** (1993) 310.
[35] (a) *D. Girton, S. Kwiatowski, G. F. Lipscomb, and R. Lytel:* Appl. Phys. Lett. **58** (1991) 1730.
(b) *C. C. Teng:* Appl. Phys. Lett. **60** (1992) 1538.
(c) *T. Findakly and C. C. Teng:* Proc. SPIE **2025** (1993) 526.
(d) *B. A. Smith, M. Jurich, W. E. Moerner, and W. Volksen:* Proc. SPIE **2025** (1993) 499.
(e) *J. J. Thackara, G. C. Bjorklund, W. Fleming, M. Jurich, B. A. Smith, and J. D. Swalen:* Proc. SPIE **2025** (1993) 564.
(f) *T. A. Tumolillo, Jr., and P. R. Ashley:* Proc. SPIE **2025** (1993) 488.
[36] *S. Yamada, Y. M. Cai, R. F. Shi, M. H. Wu, W. D. Chen, Q. M. Qian, and A. F. Garito:* Proc. Mat. Res. Soc. **328** (1994) 523.

Table 1. Comparison of key features of E-O modulators

	Mach-Zehnder interferometer	Birefringent modulator	Directional coupler
r_{eff}	r_{33} or r_{13}	r_{33}-r_{13}	r_{33} or r_{13}
V_π	low $V_{\pi MZ}$	medium 1.5 x $V_{\pi MZ}$	high 1.73 x $V_{\pi MZ}$
modulation power	low P_{MZ}	medium 1.25 x P_{MZ}	high 3 x P_{MZ}
harmonic distortion	odd terms	odd terms	all terms

Table 1. Comparison of key features of E-O modulators

	Mach-Zehnder interferometer	Birefringent modulator	Directional coupler
r_{eff}	r_{33} or r_{13}	r_{33}-r_{13}	r_{33} or r_{13}
$V\pi$	low $V_{\pi MZ}$	medium 1.5 x $V_{\pi MZ}$	high 1.73 x $V_{\pi MZ}$
modulation power	low P_{MZ}	medium 1.25 x P_{MZ}	high 3 x P_{MZ}
harmonic distortion	odd terms	odd terms	all terms

Table 2. Critical parameters characterizing electro-optic modulators

Velocity Mismatch	$L_{max}f_m = c/2(n - \sqrt{\varepsilon_{eff}})$	
	GaAs	$LiNbO_3$
	40 GHz-cm	6 GHz-cm
Modulation Efficiency	$(\phi/E_m)(\lambda_0/\lambda_m) = n^3r/(n - \sqrt{\varepsilon_{eff}})$	
	GaAs	$LiNbO_3$
	1.7×10^{-4}	1.3×10^{-4}

Table 3. Temperature requirements for opto-electronic integration

Operation (Long Term)	-40 to 125°C (Military Specification) 20 to 100°C (Commercial)
Processing & Packaging (Short Term, 1-10 minutes)	
Wire Bonding	100 to 150°C
Solder Bonding	150 to 200°C
Hermetic Packaging	150 to 250°C

FIGURE CAPTIONS

Fig. 1. Common electro-optic modulator configurations are illustrated. (a) A simple schematic representation of a Mach-Zehnder interferometer is given. (b) A birefringent modulator is shown. (c) A directional coupler integrated into a fiber optic network is shown; this figure also illustrates key features of the integration process such as the fiber optic cable to modulator waveguide transition.

Fig. 2. The half-wave voltage-modulation length product of a $LiNbO_3$ modulator and a polymer modulator (with a hypothetical E-O coefficient of 100 pm/V) are shown as a function of frequency.

Fig. 3. Representative NLO chromophores are shown together with their $\mu\beta$ values and decomposition temperatures (where available). Chromophore c was prepared by Garito and coworkers [13a]. Chromophore b was prepared by the IBM-Almaden research group [11b,11c,29]. Chromophores f and g are from the Ph.D. thesis of C. Xu (USC, 1993). For other chromophores see [20b].

Fig. 4. Two schemes for producing hardened NLO lattices are shown. On the left hand side, prepolymer preparation and lattice hardening are accomplished by functionalities, with different (e.g., addition and condensation) reactivities, which terminate the donor and acceptor ends of an NLO chromophore. For example, the acceptor end of the chromophore may contain a acrylate functionality which is capable of undergoing addition polymerization while the donor end may contain hydroxyl groups capable of undergoing condensation reactions. With this scheme, the intermediate prepolymer typically contains the NLO chromophore as a pendant to the polymer main chain. The right hand side illustrates the use of chromophore where the donor and acceptor ends of the chromophore are terminated with the same functionality, e.g., hydroxyl groups capable of undergoing condensation reactions. In this case, the prepolymer contains the NLO chromophore as a component of the polymer main chain. At the bottom, we show two representative chromophores discussed in [24a].

Fig. 5. The thermal stability (measured at 125°C) of optical nonlinearity (second harmonic generation efficiency) is shown for crosslinked and uncrosslinked samples of the chromophore shown at the bottom left of Fig. 4 [24a]. The E-O coefficient for this sample is 14 pm/V. Excellent thermal stability at 125°C is observed for both the nitro and sulfonyl chromophores of Fig. 4. The detailed conditions of crosslinking are described in [24a].

Fig. 6. A schematic representation of the apparatus used to effect a dynamic assay of thermal stability of optical nonlinearity is shown. The second harmonic generation efficiency is constantly monitored as a function of uniform heating, e.g., typically at a rate of 10°C per minute.

Fig. 7. The thermal stability of the chromophore of Fig. 5 is determined by the dynamic assay technique employing a heating rate of 10°C per minute. The conditions of synthesis and lattice incorporation of this chromophore are described in [24a].

Fig. 8. The thermal stability of a azobenzene chromophore containing an amine donor and sulfonyl acceptor is shown. This material was prepared by addition polymerization of a methacrylate functionality terminating the sulfonyl acceptor followed by a condensation crosslinking reaction involving hydroxyl groups terminating the donor end of the chromophore and isocyanate crosslinking reagents [24a]. The chromophore structure in the hardened polymer is that shown at the bottom right of Fig. 4. This chromophore exhibits no measurable loss of optical nonlinearity at 100°C for 1000 hours or 125°C for 300 hours. The step trace shown in this figure (measured by the dynamic assay method with a heating rate of 10°C per minute) is indicative of incomplete crosslinking. Various preparations yielded E-O coefficients in the range 9-13 pm/V.

Fig. 9. A scheme for the incorporation of a high $\mu\beta$ chromophore into a hardened lattice by general procedure 1 is shown.

Fig. 10. A scheme for incorporating an improved chromophore into a hardened lattice structure is shown.

Fig. 11. Two schemes for preparing hardened NLO polyimide lattices are shown.

Fig. 12. The thermal stability of optical nonlinearity (measured by the dynamic assay with a heating rate of 10°C per minute) of the NLO polyimide system of Fig. 11b is shown. Note the improvement of thermal stability (T_g elevation) associated with the imidization step.

Fig. 13. The preparation of a glass, convalently incorporating an NLO chromophore, by sol-gel processing is shown.

Fig. 14. Preparation of a hardened NLO lattice by a thermosetting reaction is shown.

Fig. 15. a.) The thermal stability data for the hardened lattice in Fig. 13 are provided. b.) Thermal stability data for the hardened polymer lattice in Fig. 14 are shown.

Fig. 16. Fabrication of a buried channel NLO waveguide by two-color photochemical processing is shown. a.) The two step (two color) processing scheme is illustrated together with a schematic representation of the index variation. b.) Index of refraction and optical mode profiles are shown for the above processing scheme for the polymer of Fig. 14.

Fig. 17. a.) The steps involved in preparing a buried channel NLO waveguide by reactive ion etching are illustrated. b.) The accuracy of the etch depth to assure single mode propagation for the polyimide structure of Fig. 11b is shown. Points falling above the curve are multi-mode; those below the curve are single mode.

Fig. 18. A schematic representation of a birefringent modulator and associated test bed is shown.

Fig. 19. A scheme for pigtailing an organic electro-optic modulator to fiber optic transmission lines is shown.

Fig. 20. a.) Oscilloscope traces of a low frequency modulation signal (top) and the electrical drive signal (bottom) are shown. b.) Measurement of V_π is shown. c.) A spectrum analyzer scan, detecting 400 MHz modulation, is shown. The sample is an NLO polyurethane prepared by a thermosetting scheme (see Fig. 14).

A

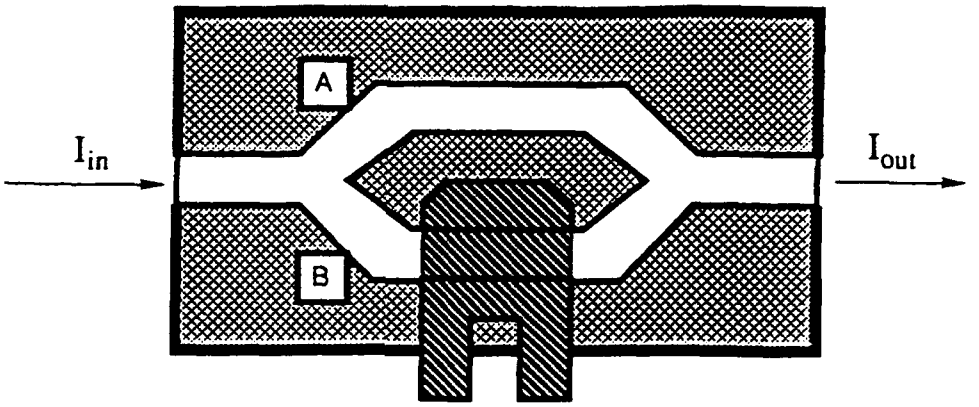
A
B
I_{in}
I_{out}
Applied Voltage

B

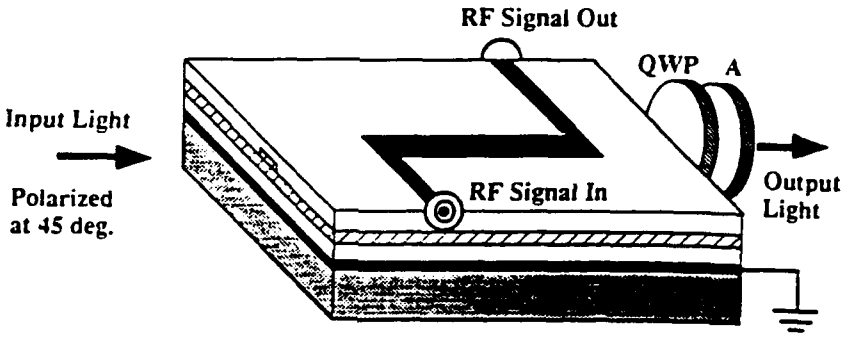
RF Signal Out
QWP
A
Input Light
Polarized at 45 deg.
RF Signal In
Output Light

C

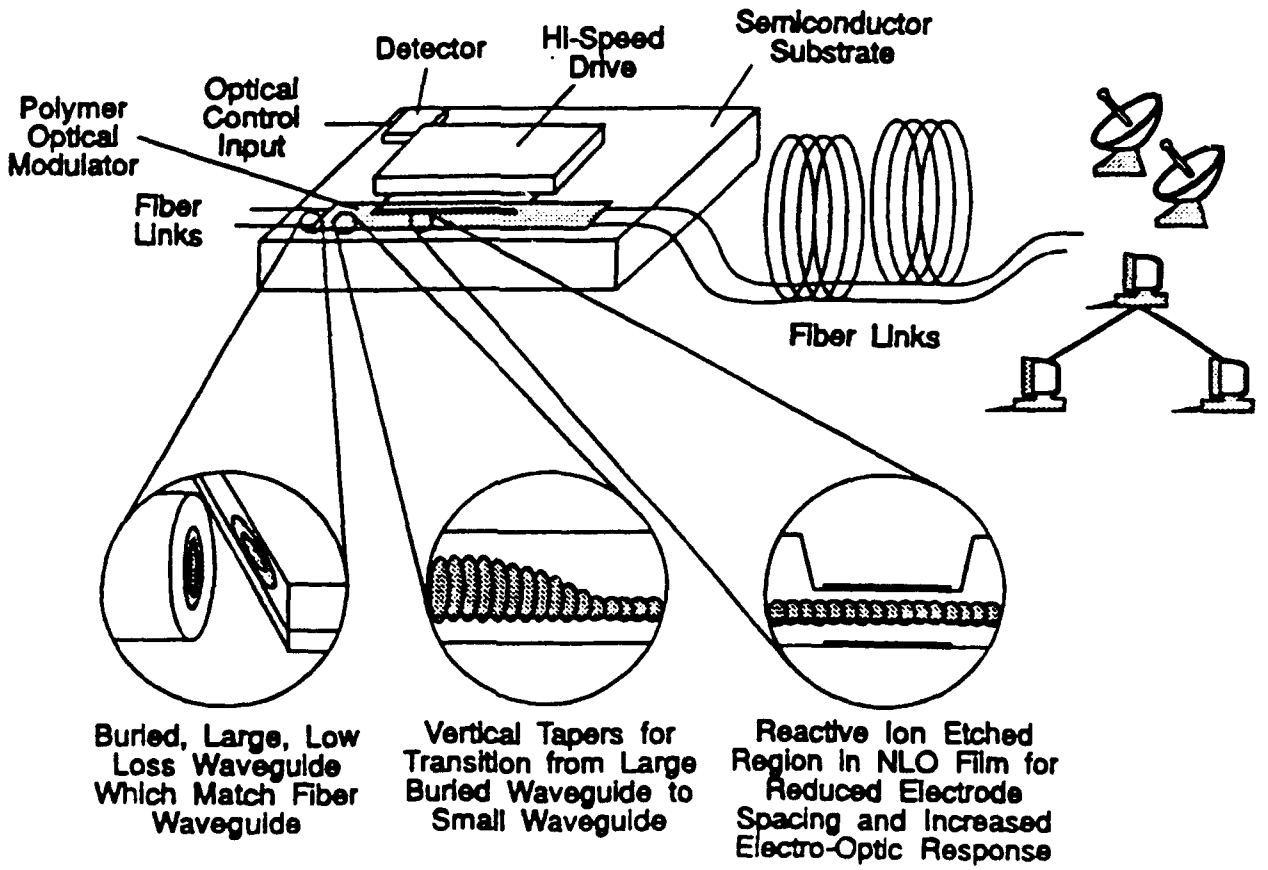
Detector
Hi-Speed Drive
Semiconductor Substrate
Polymer Optical Modulator
Optical Control Input
Fiber Links
Fiber Links
Buried, Large, Low Loss Waveguide Which Match Fiber Waveguide
Vertical Tapers for Transition from Large Buried Waveguide to Small Waveguide
Reactive Ion Etched Region in NLO Film for Reduced Electrode Spacing and Increased Electro-Optic Response

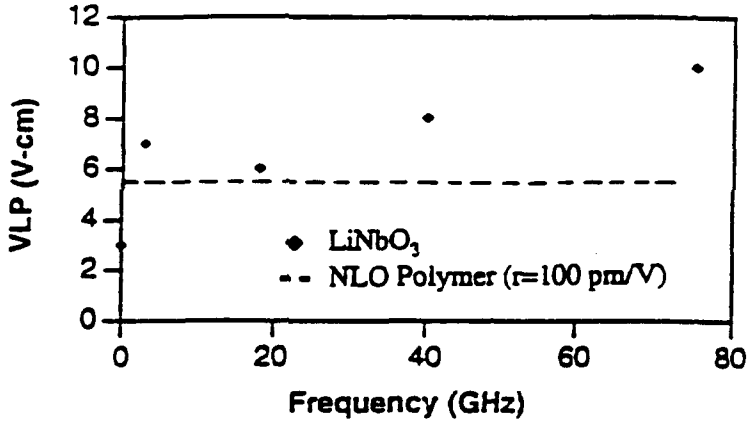
12
10
8
6
4
2
0
VLP (V-cm)
0
20
40
60
80
Frequency (GHz)
LiNbO3
NLO Polymer (r=100 pm/V)

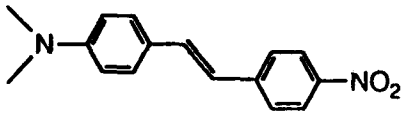

$\mu\beta$ (0) = 1, T_d = 290°C

a

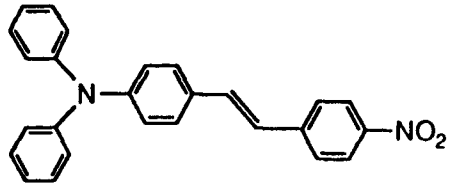

$\mu\beta$ (0) =0.6, T_d = 358°C

b

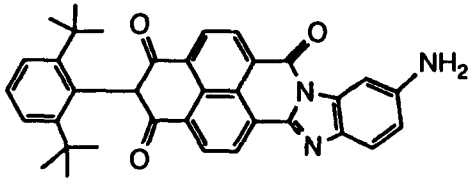

$\mu\beta$ (0) ~ 1, T_d > 350°C

c

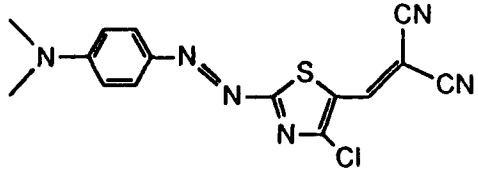

$\mu\beta$ (0) ~ 4-5

d

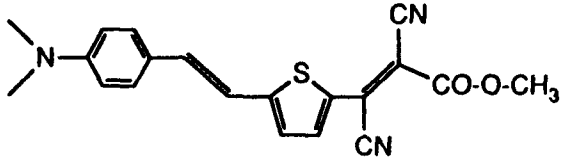

$\mu\beta$ (0) ~ 4-5

e

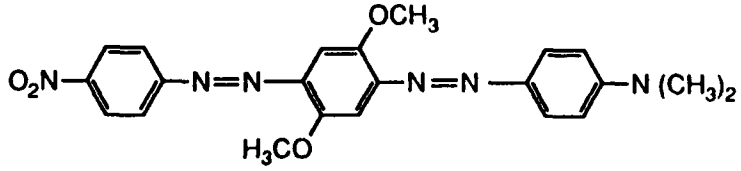

$\mu\beta$(0) ~ 3, T_d = 275°C

f

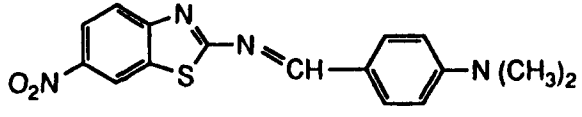

$\mu\beta$(0) ~ 2, T_d = 330°C

g

A)

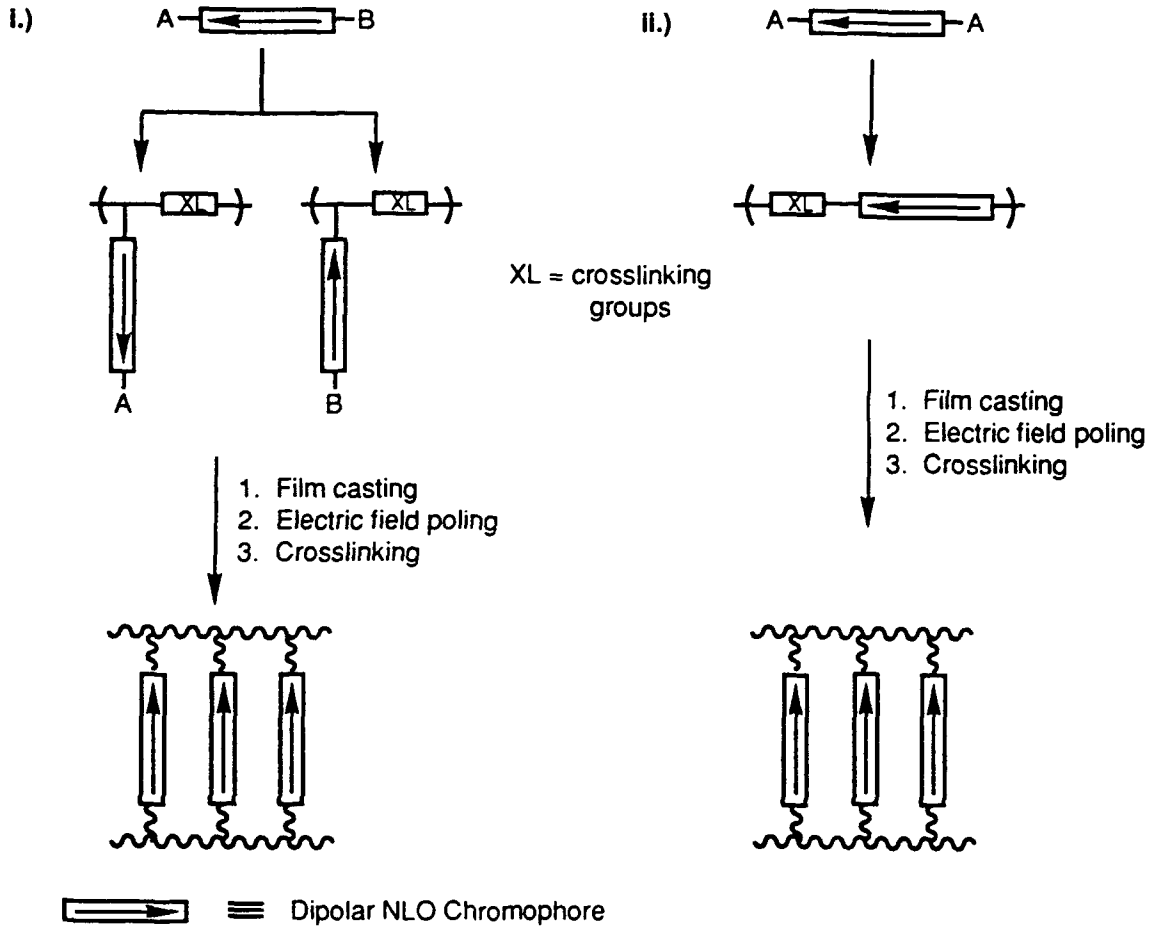
i.)
A
B
XL
XL
A
B
1. Film casting
2. Electric field poling
3. Crosslinking
ii.)
A
A
XL
XL = crosslinking groups
1. Film casting
2. Electric field poling
3. Crosslinking
Dipolar NLO Chromophore

B)

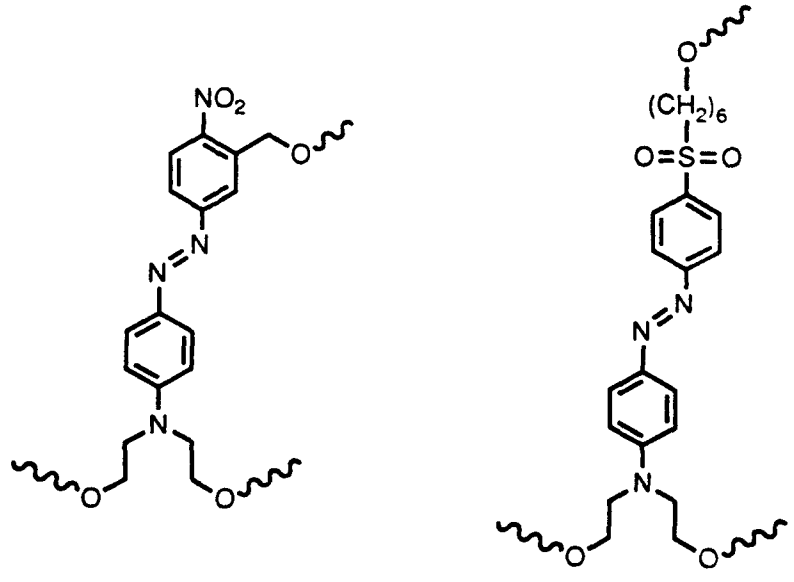
NO2
N
N
N
O
O
O
(CH2)6
O=S=O
N
N
N
O
O

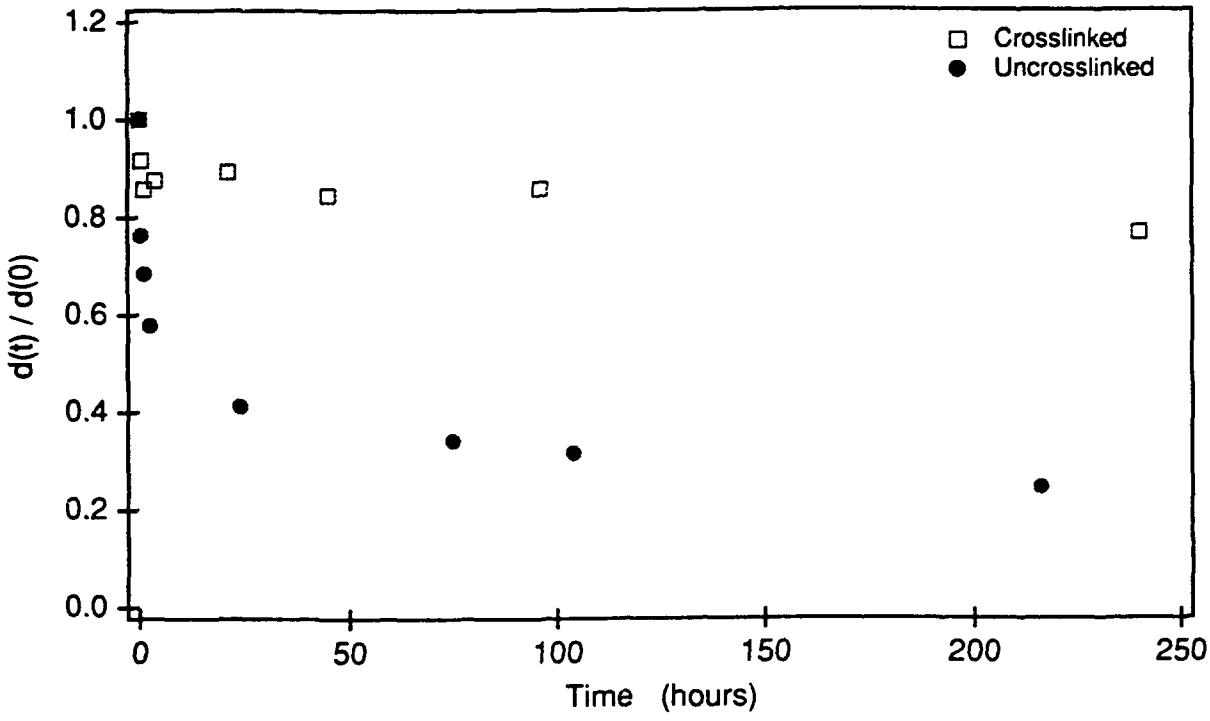
Crosslinked
Uncrosslinked
d(t) / d(0)
1.2
1.0
0.8
0.6
0.4
0.2
0.0
0
50
100
150
200
250
Time (hours)

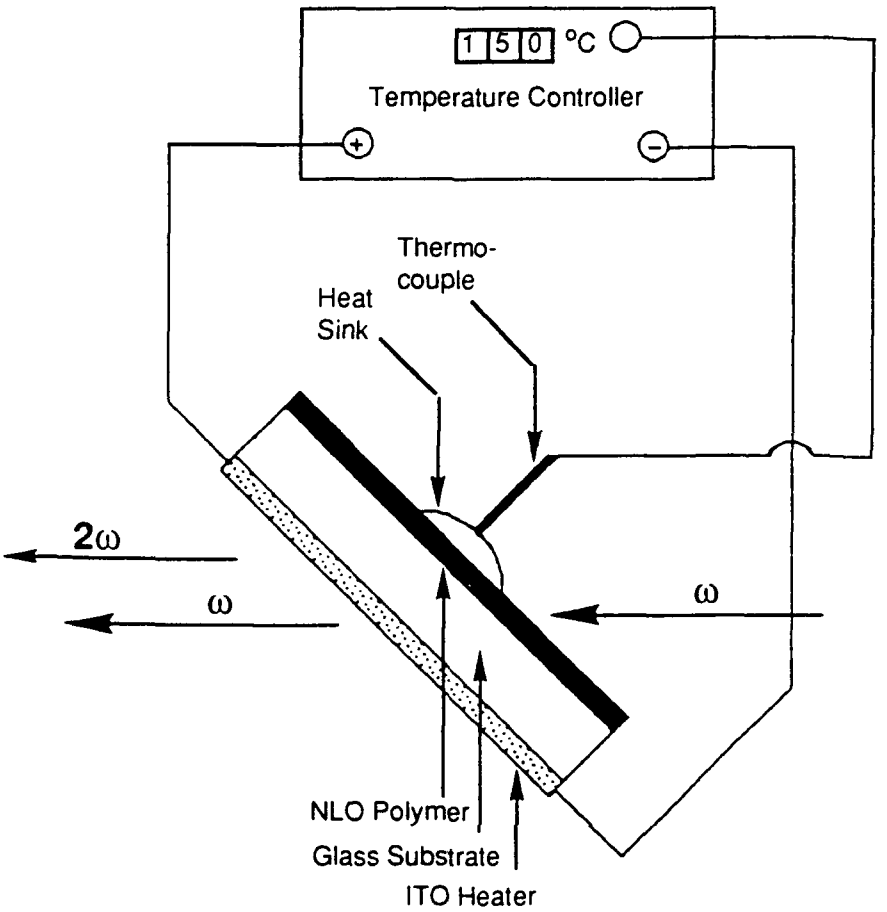
1 5 0 °C
Temperature Controller
Thermo-
couple
Heat
Sink
2ω
ω
ω
NLO Polymer
Glass Substrate
ITO Heater

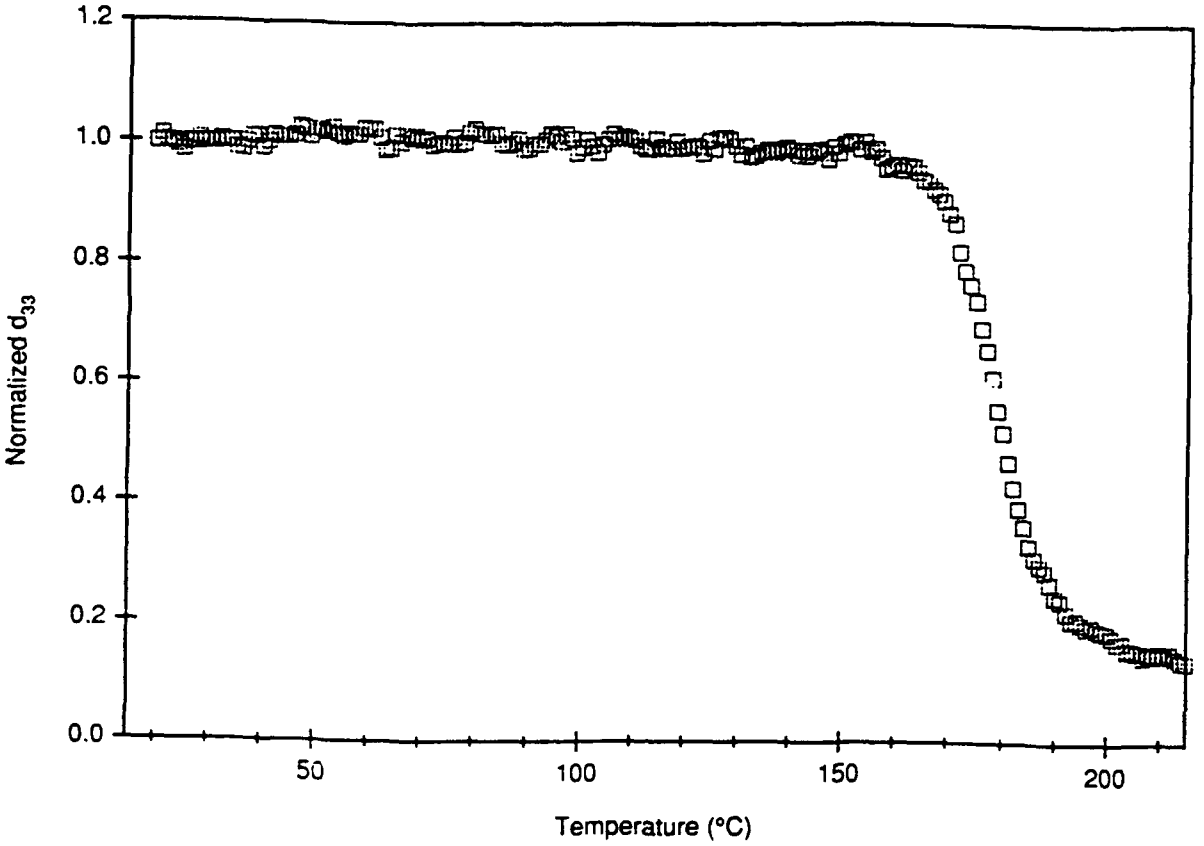
1.2
1.0
0.8
0.6
0.4
0.2
0.0
Normalized d_{33}
50
100
150
200
Temperature (°C)

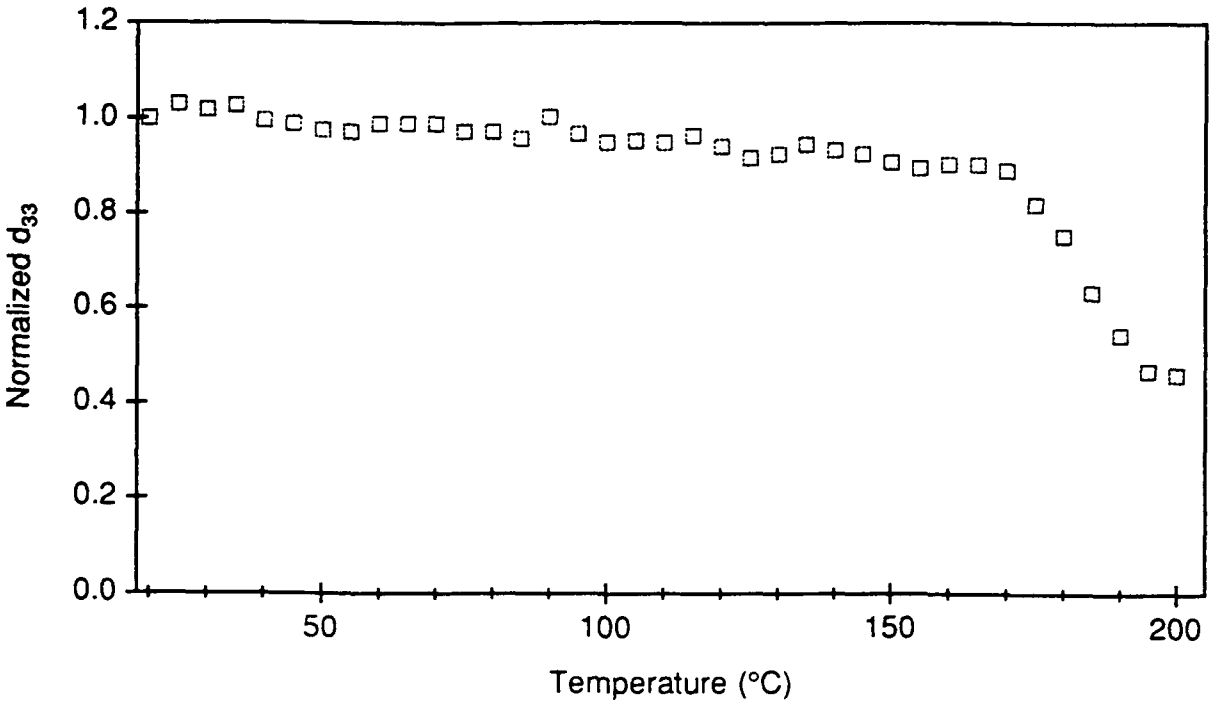
1.2
1.0
0.8
0.6
0.4
0.2
0.0
Normalized d_{33}
50
100
150
200
Temperature (°C)

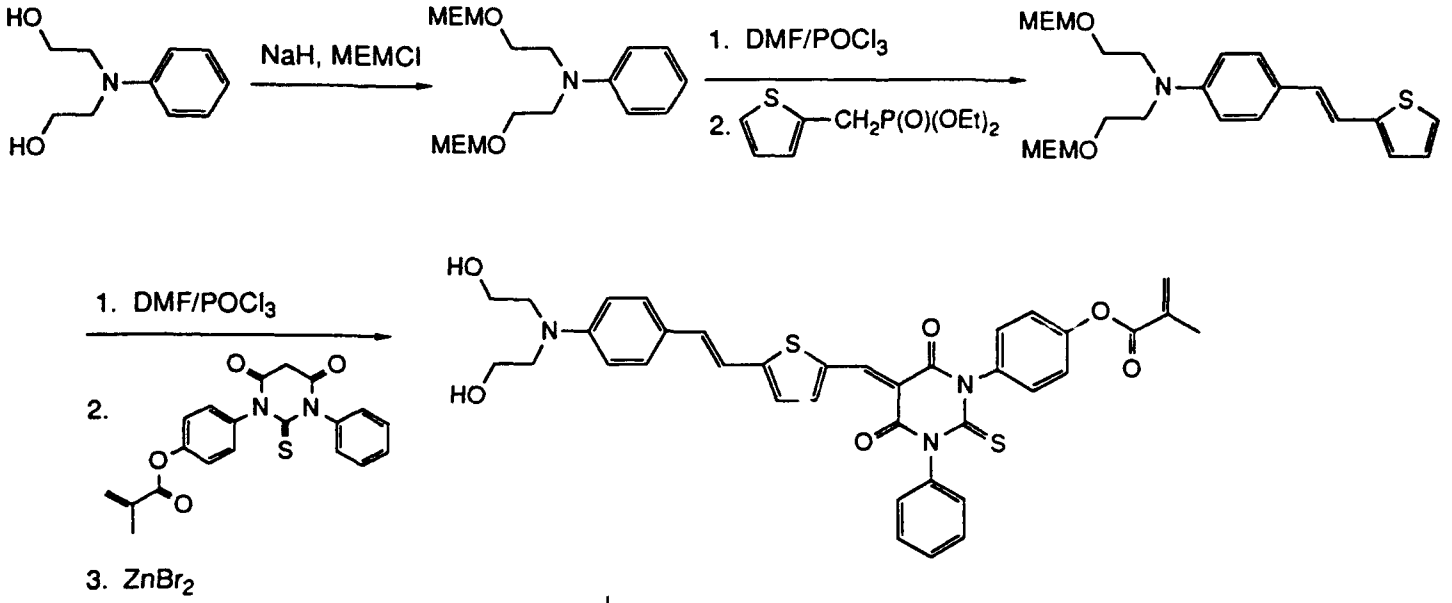

copolymerize with methyl methacrylate and hydroxyethyl methacrylate

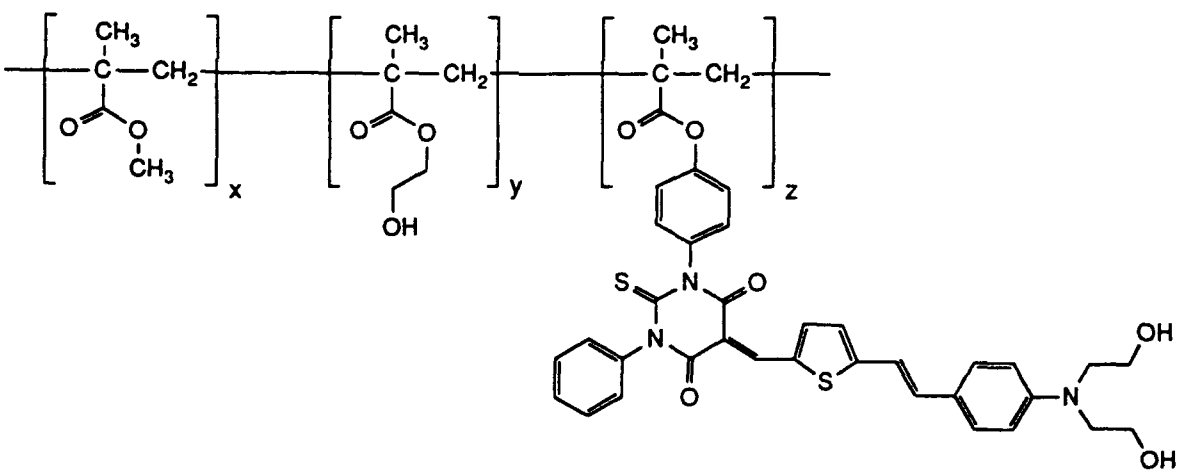

1. cast into film with 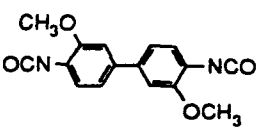

2. electric field poling

3. heat to effect crosslinking

heavily crosslinked 3D network

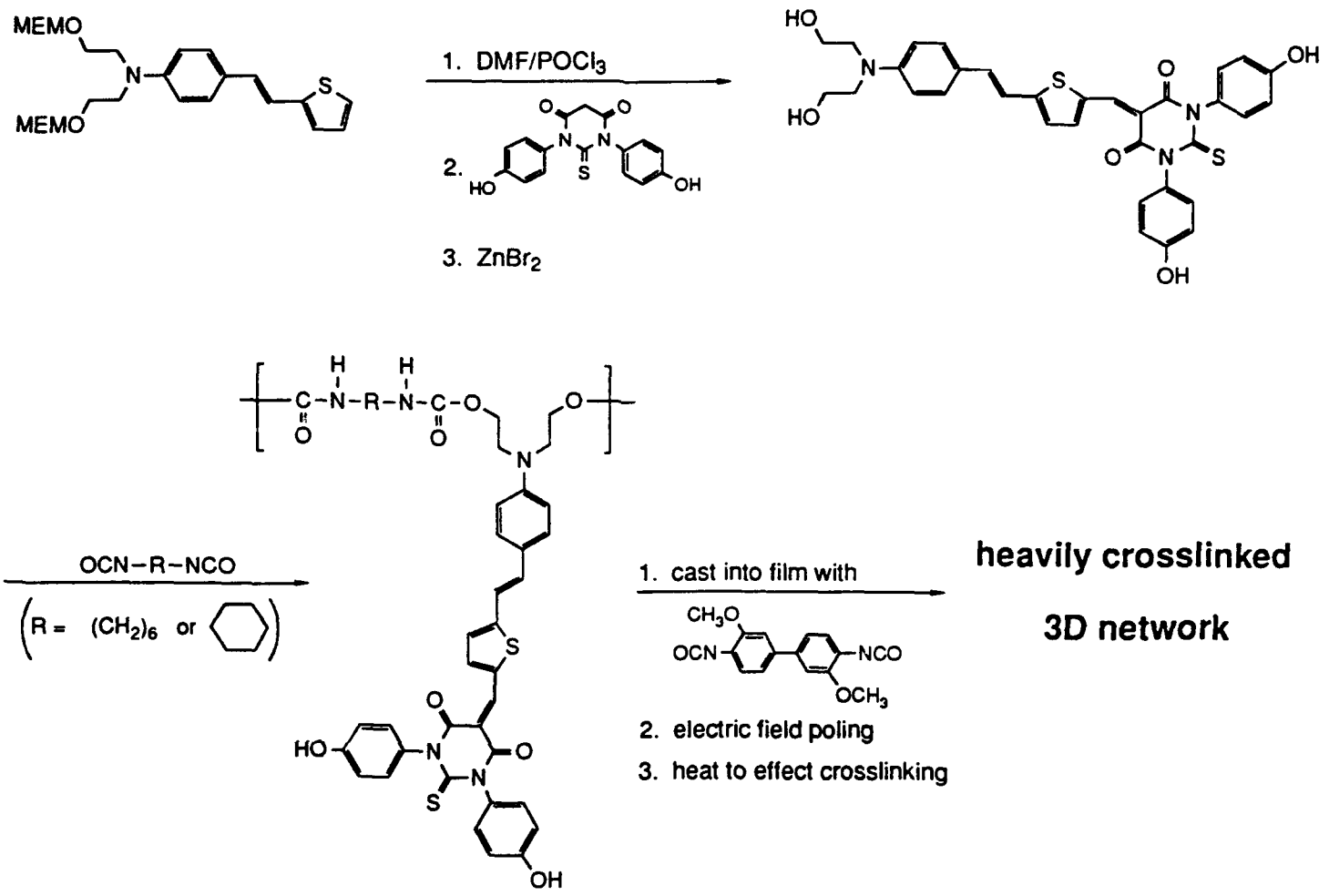
MEMO
MEMO
1. DMF/POCl3
2.
3. ZnBr2
HO
HO
OH
OH
OCN–R–NCO
(R = (CH2)6 or
1. cast into film with
CH3O
OCN
NCO
OCH3
2. electric field poling
3. heat to effect crosslinking
heavily crosslinked
3D network

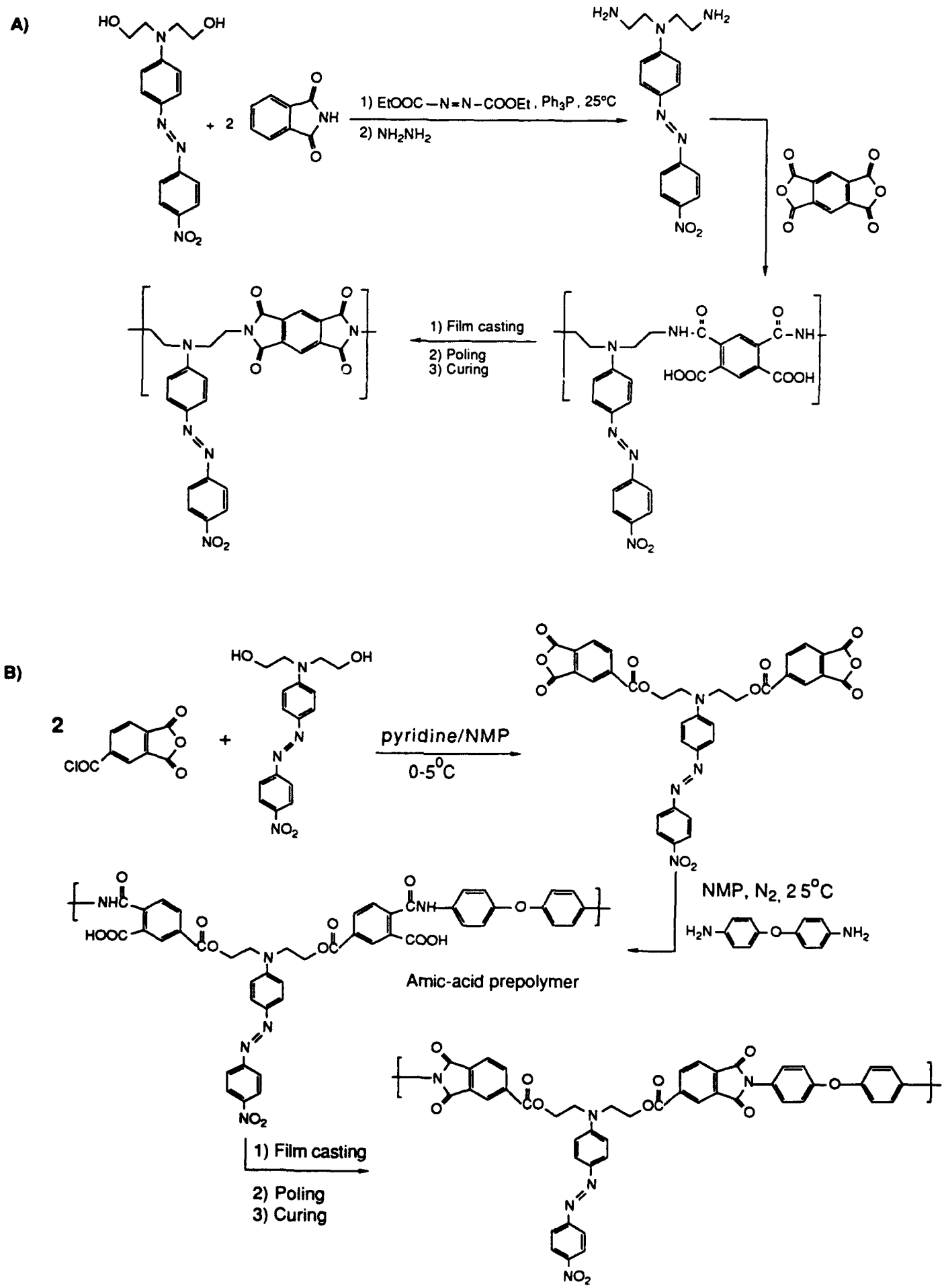
A)
HO
OH
N
N
N
NO2
+ 2
NH
O
1) EtOOC—N=N—COOEt , Ph3P , 25°C
2) NH2NH2
H2N
NH2
1) Film casting
2) Poling
3) Curing
NH-C
C-NH
HOOC
COOH
B)
2
ClOC
pyridine/NMP
0-5°C
NMP, N2, 25°C
Amic-acid prepolymer
1) Film casting
2) Poling
3) Curing

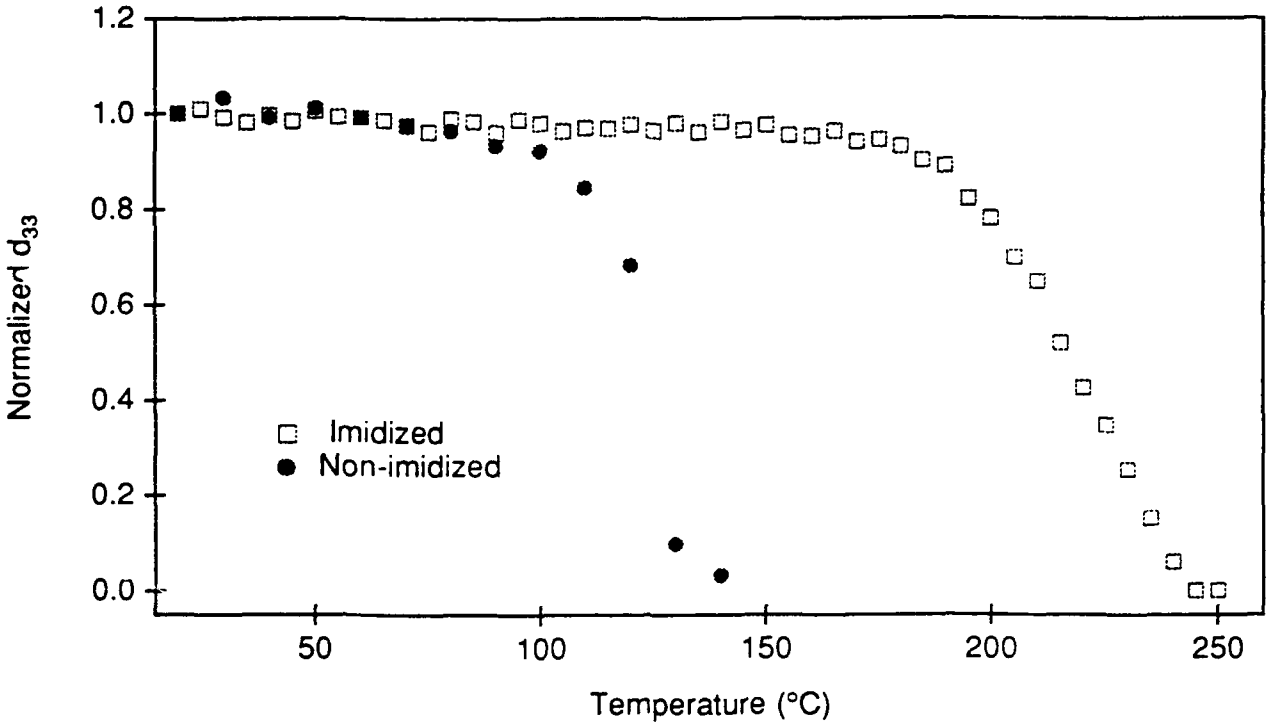
1.2
1.0
0.8
0.6
0.4
0.2
0.0
Normalized d_{33}
Imidized
Non-imidized
50
100
150
200
250
Temperature (°C)

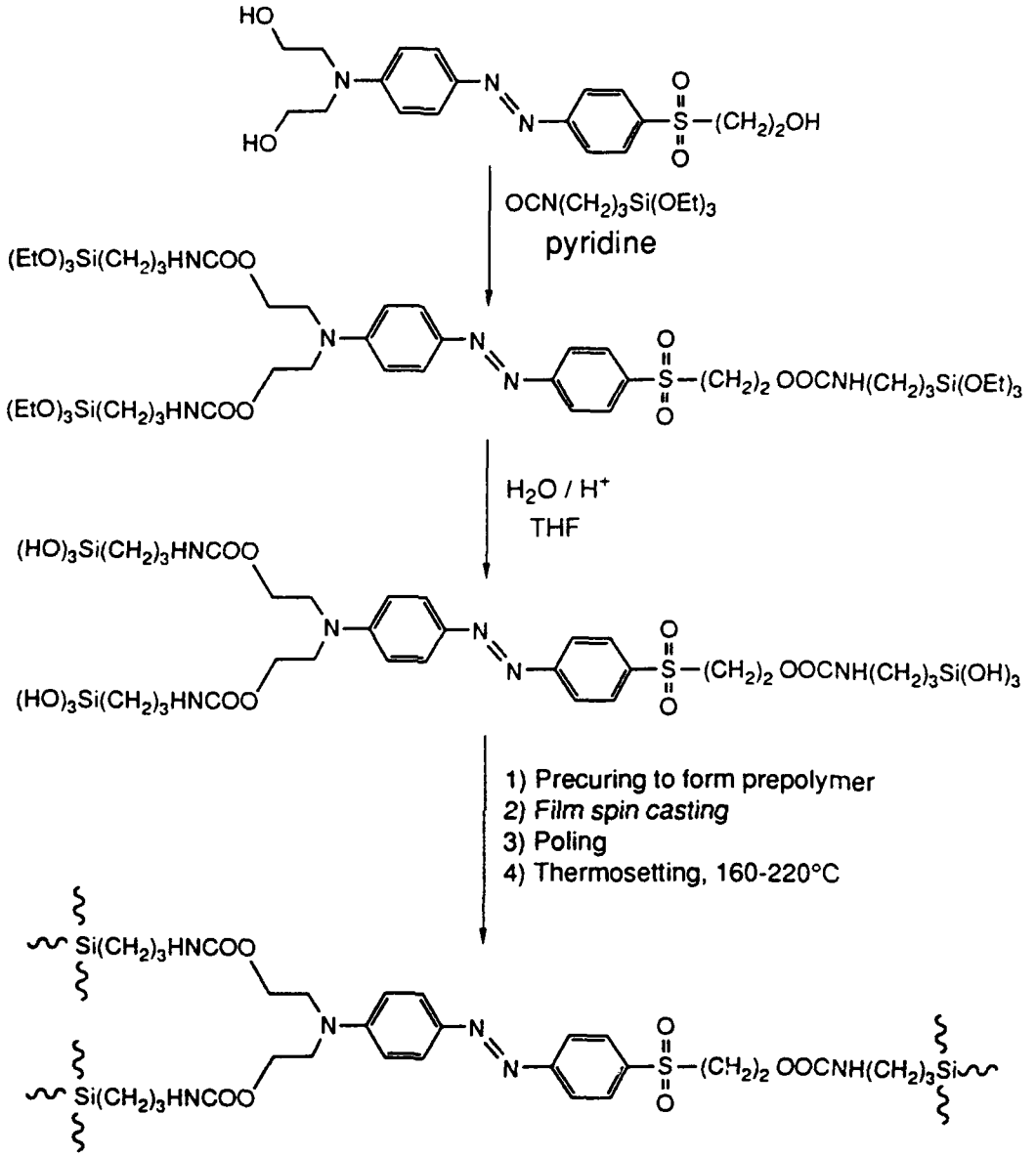

3D network with dipole alignment locked in

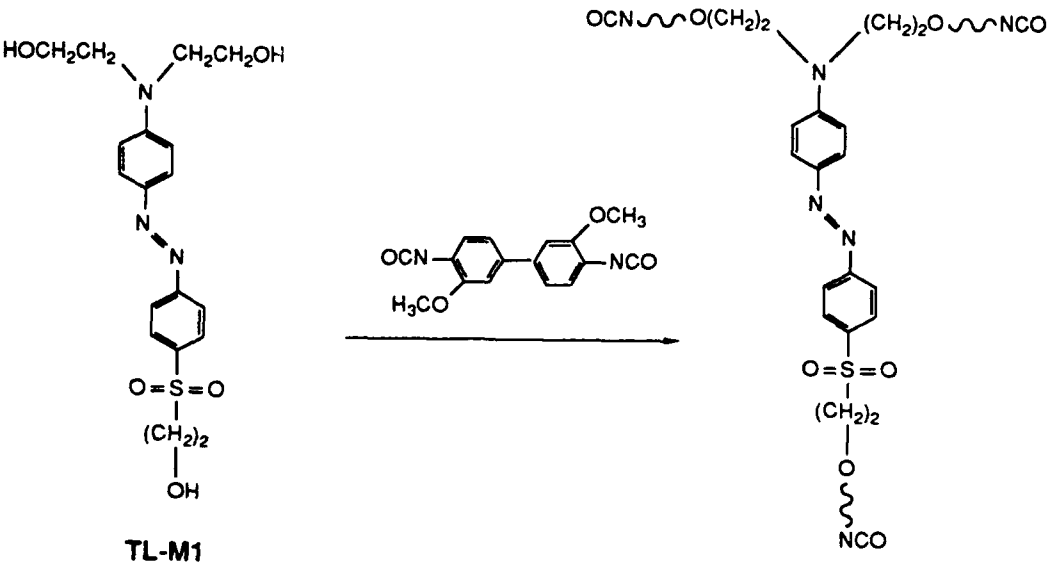

TL-M1

TL-M2

TL-M1 + TL-M2 → (1) Precuring, (2) Film casting, (3) Electric poling, (4) Thermosetting → **3D Network**

A)

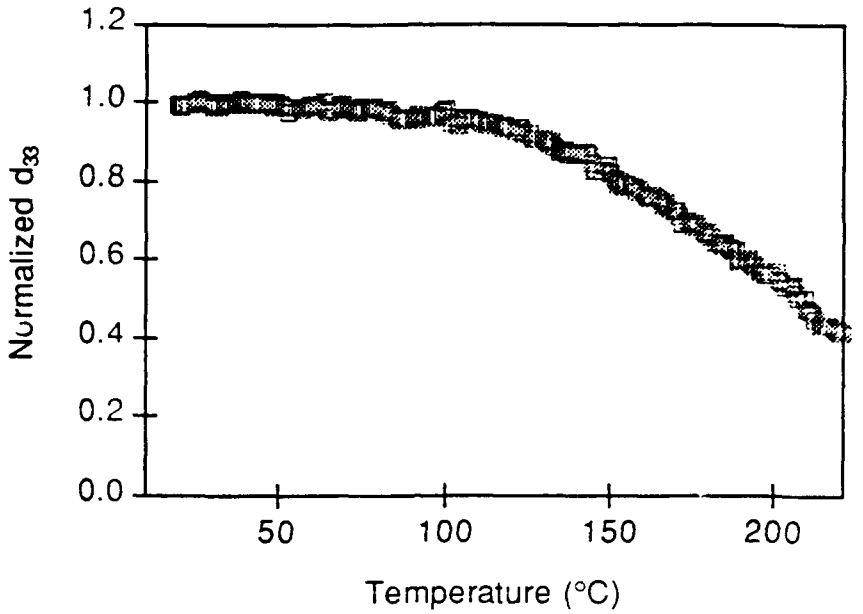
1.2
1.0
0.8
0.6
0.4
0.2
0.0
Normalized d_{33}
50
100
150
200
Temperature (°C)

B)

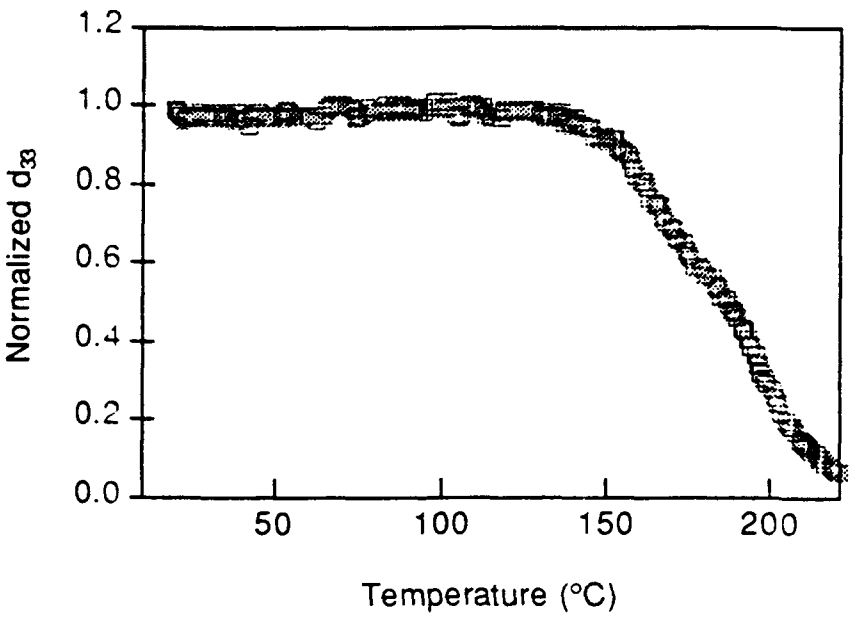
1.2
1.0
0.8
0.6
0.4
0.2
0.0
Normalized d_{33}
50
100
150
200
Temperature (°C)

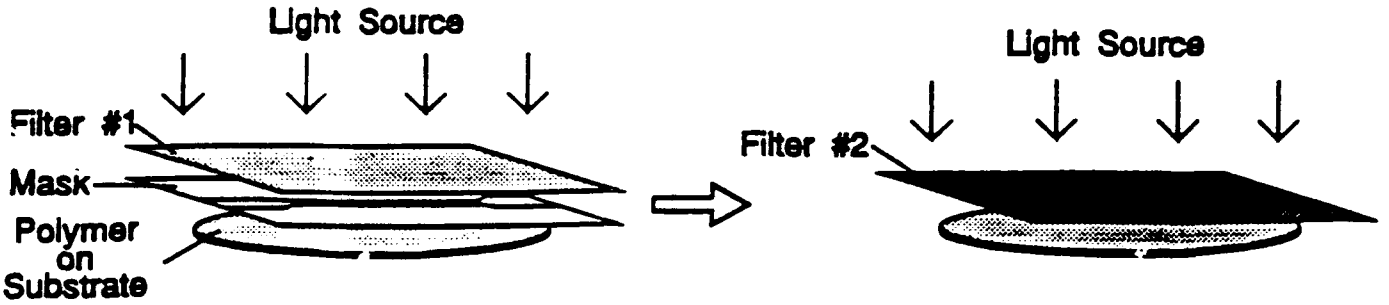

A

Small Δn gradients (large mode size)
Buried single-mode waveguides
All optical processing using standard lithography
Single cladding layer
Reduced thin film stresses
Reduced processing and higher yields

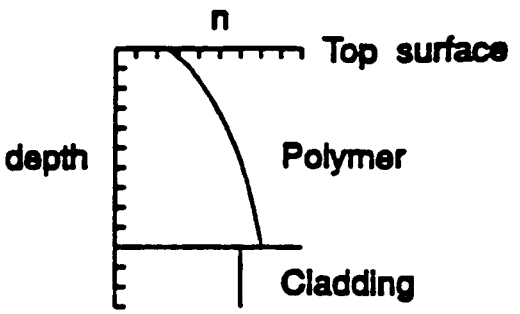

B

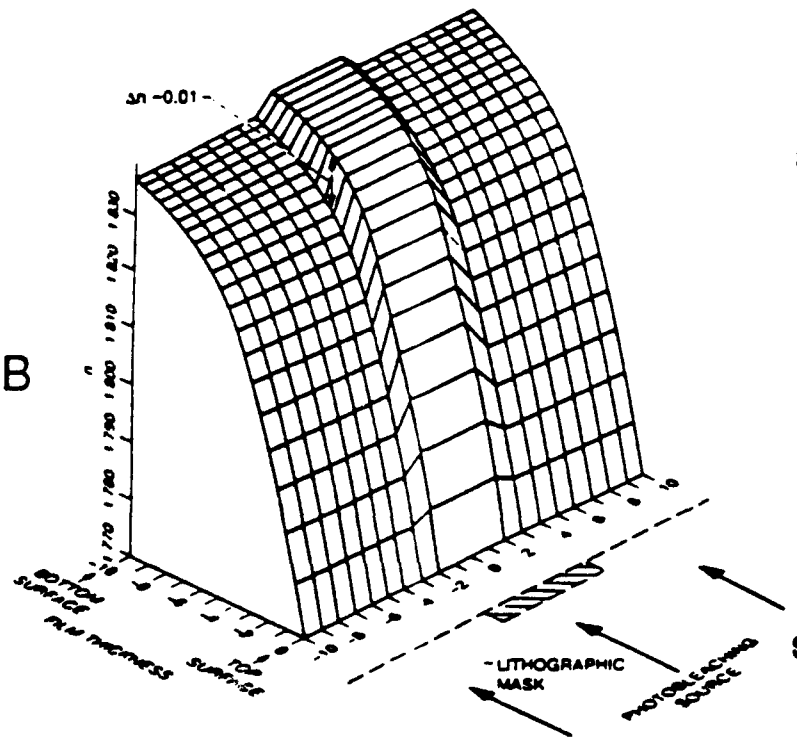

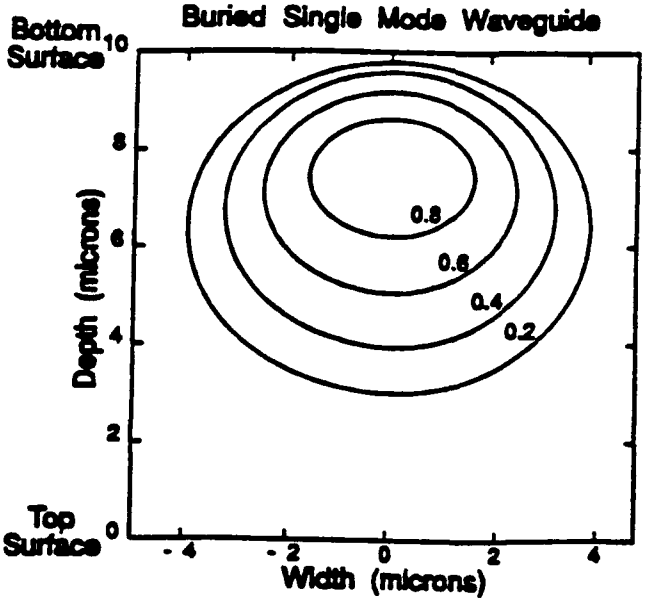

A

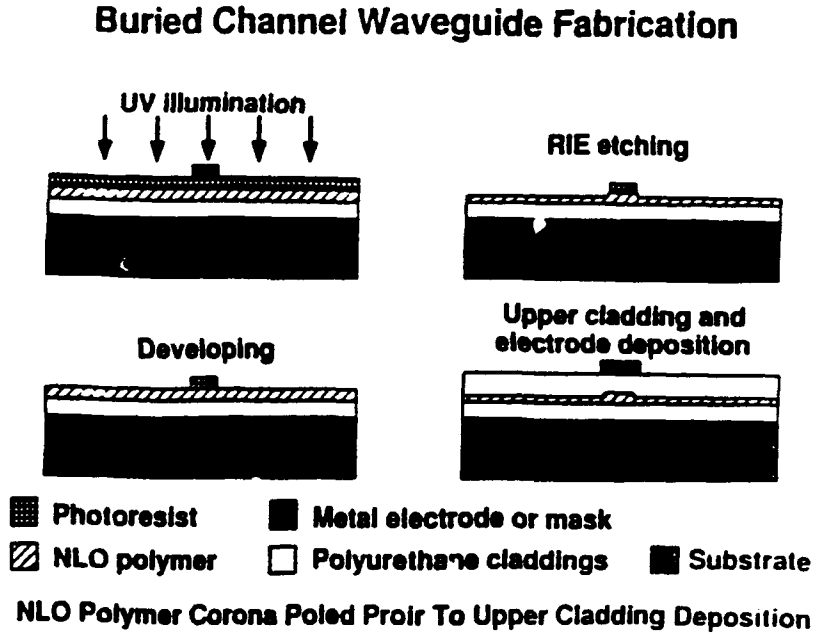
Buried Channel Waveguide Fabrication
UV illumination
RIE etching
Developing
Upper cladding and electrode deposition
Photoresist
Metal electrode or mask
NLO polymer
Polyurethane claddings
Substrate
NLO Polymer Corona Poled Prior To Upper Cladding Deposition

B

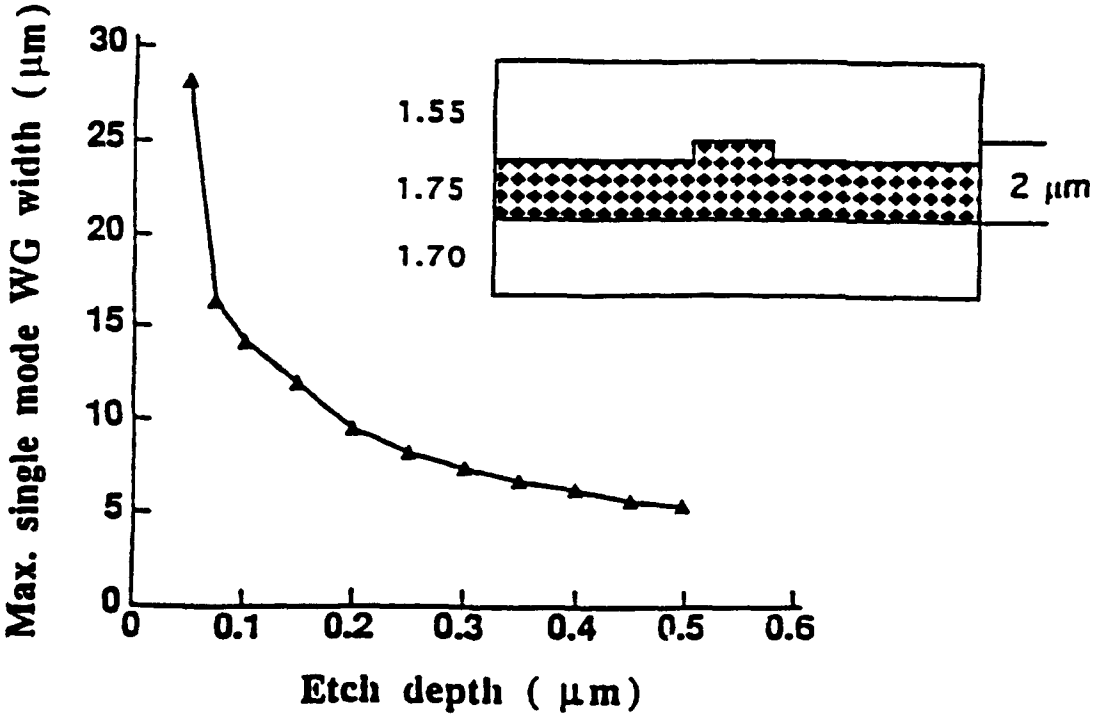
Max. single mode WG width (μm)
30
25
20
15
10
5
0
0
0.1
0.2
0.3
0.4
0.5
0.6
Etch depth (μm)
1.55
1.75
1.70
2 μm

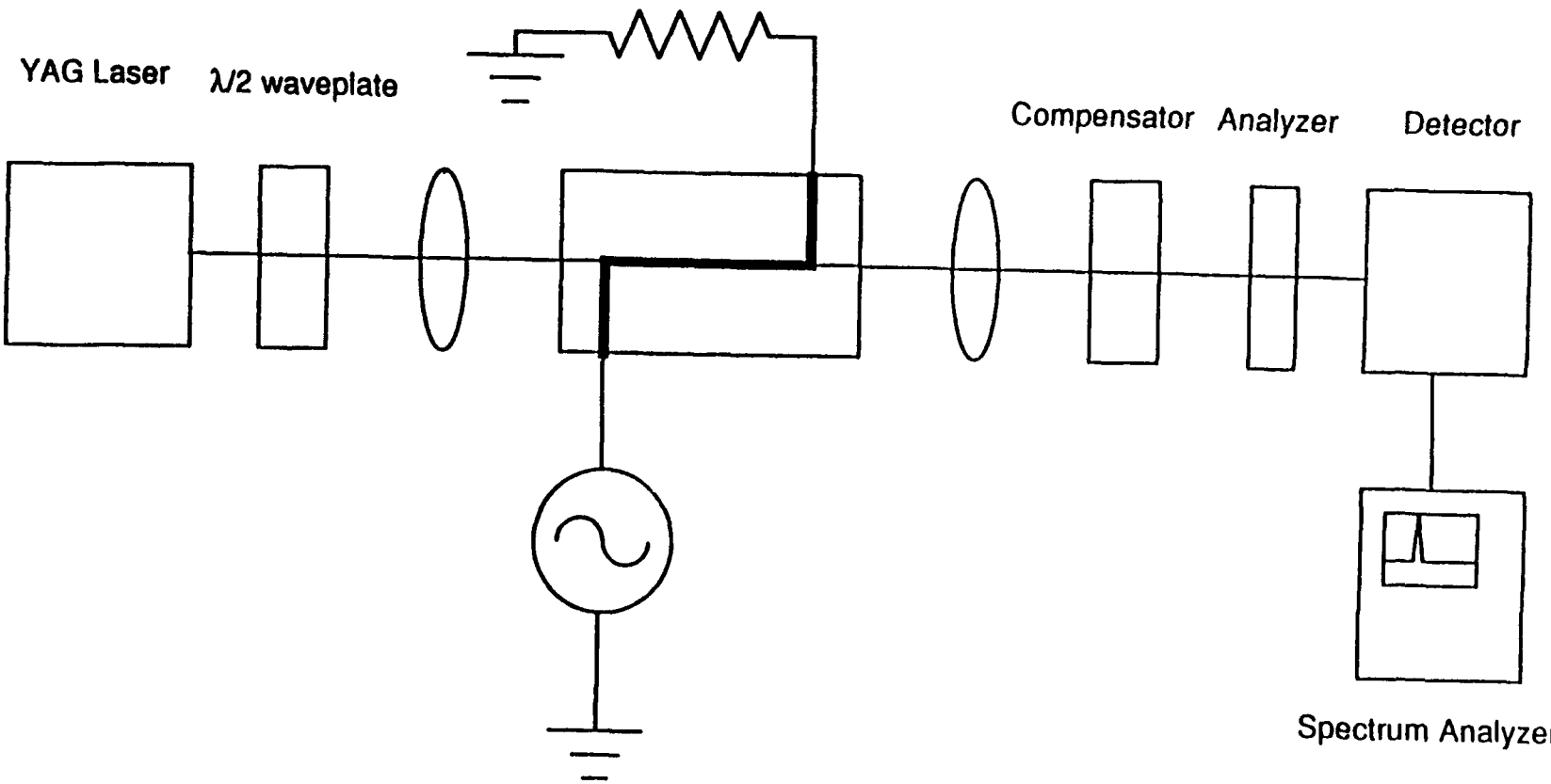
YAG Laser
λ/2 waveplate
Compensator
Analyzer
Detector
Spectrum Analyzer

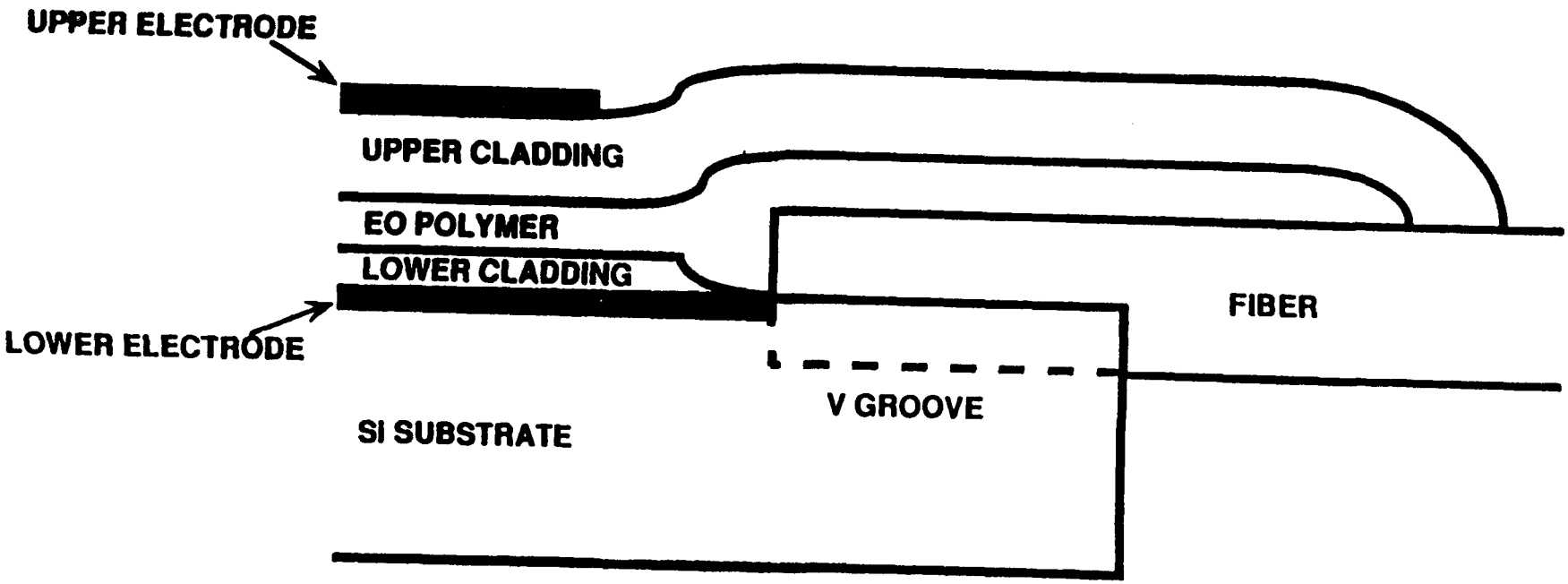
UPPER ELECTRODE
UPPER CLADDING
EO POLYMER
LOWER CLADDING
LOWER ELECTRODE
FIBER
V GROOVE
SI SUBSTRATE

A

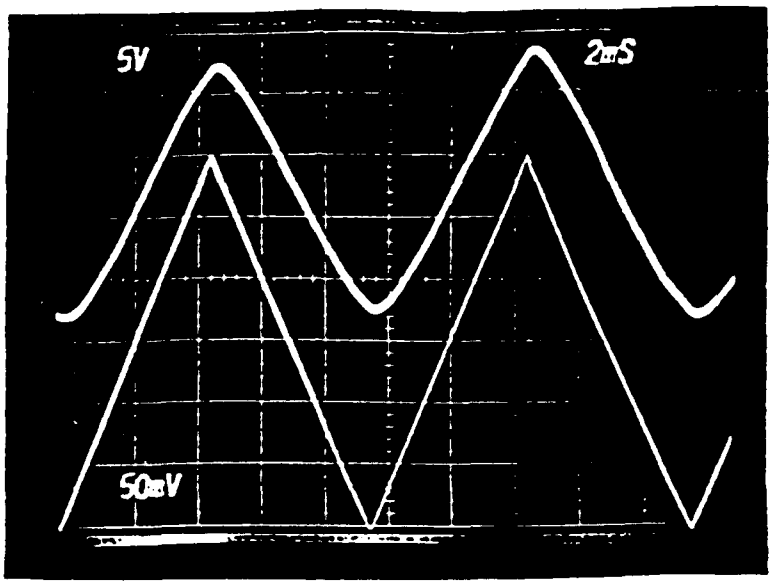

B

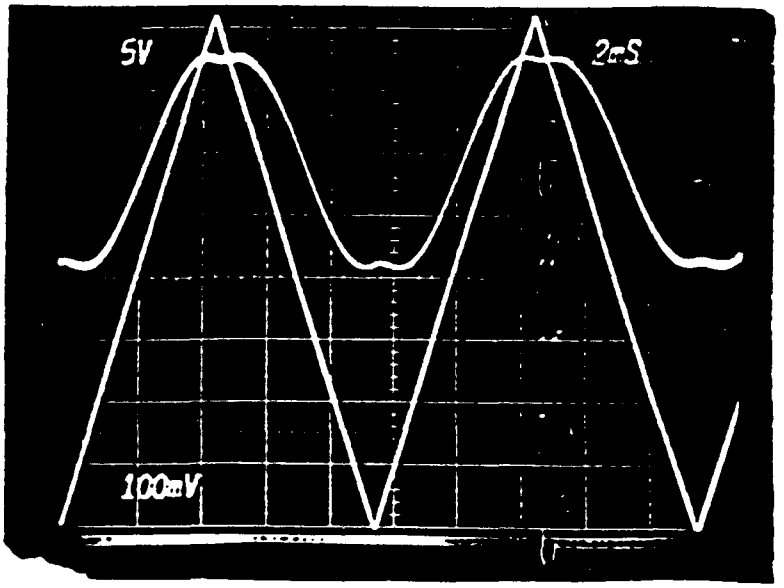

C